Histone H4 Facilitates the Proteolysis of the Budding Yeast CENP-A^{Cse4} Centromeric Histone Variant

Gary M. R. Deyter,*,†,1 Erica M. Hildebrand,*,‡,1 Adrienne D. Barber,* and Sue Biggins*,2

*Howard Hughes Medical Institute, Division of Basic Sciences, Fred Hutchinson Cancer Research Center, Seattle, Washington 98040, †Department of Health Services Research, University of Texas MD Anderson Cancer Center, Houston, Texas 77030, and ‡Molecular and Cellular Biology Program, University of Washington, Seattle, Washington 98195

ORCID ID: 0000-0002-4499-6319 (S.B.)

ABSTRACT The incorporation of histone variants into nucleosomes can alter chromatin-based processes. CENP-A is the histone H3 variant found exclusively at centromeres that serves as an epigenetic mark for centromere identity and is required for kinetochore assembly. CENP-A mislocalization to ectopic sites appears to contribute to genomic instability, transcriptional misregulation, and tumorigenesis, so mechanisms exist to ensure its exclusive localization to centromeres. One conserved process is proteolysis, which is mediated by the Psh1 E3 ubiquitin ligase in *Saccharomyces cerevisiae* (budding yeast). To determine whether there are features of the CENP-A nucleosome that facilitate proteolysis, we performed a genetic screen to identify histone H4 residues that regulate CENP-A^{Cse4} degradation. We found that H4-R36 is a key residue that promotes the interaction between CENP-A^{Cse4} and Psh1. Consistent with this, CENP-A^{Cse4} protein levels are stabilized in H4-R36A mutant cells and CENP-A^{Cse4} is enriched in the euchromatin. We propose that the defects in CENP-A^{Cse4} proteolysis may be related to changes in Psh1 localization, as Psh1 becomes enriched at some 3′ intergenic regions in H4-R36A mutant cells. Together, these data reveal a key residue in histone H4 that is important for efficient CENP-A^{Cse4} degradation, likely by facilitating the interaction between Psh1 and CENP-A^{Cse4}.

KEYWORDS CENP-A^{Cse4}; H4; Psh1; proteolysis; centromere; nucleosome

CHROMATIN structure is a barrier to many processes that must gain access to DNA to generate the biomolecules required for cellular viability (Venkatesh and Workman 2015). Chromatin also serves as a platform that promotes the association of supramolecular structures with DNA, such as kinetochores that form on centromeres and capping structures that assemble at telomeres (Verdaasdonk and Bloom 2011; Kupiec 2014). The foundation of chromatin is histones, which associate with and compact DNA. Histones are therefore subject to a variety of regulatory processes, such as post-translational modifications and regulated incorporation or removal at various genomic regions (Rando and Winston 2012). Chromatin is also regulated by the deposition of histone variants, which can alter chromatin structure and accessibility to regulate cellular processes (Li and Fang 2015). One conserved histone is the H3 variant CENP-A, which localizes to centromeres to mediate their epigenetic propagation and to serve as the foundation for kinetochore assembly (Palmer *et al.* 1987; Van Hooser *et al.* 2001; Black and Cleveland 2011; Verdaasdonk and Bloom 2011). Consistent with this, CENP-A mislocalization to euchromatin can lead to ectopic kinetochore formation, genome instability, and transcriptional misregulation (Tomonaga *et al.* 2003; Heun *et al.* 2006; Amato *et al.* 2009; Hildebrand and Biggins 2016). It is therefore essential that CENP-A exclusively localizes to centromeres and does not stably incorporate into euchromatin.

One conserved mechanism that prevents ectopic CENP-A localization is ubiquitin-mediated proteolysis (Lomonte *et al.* 2001; Collins *et al.* 2004; Moreno-Moreno *et al.* 2006, 2011; Gross *et al.* 2012). The most detailed understanding of CENP-A proteolysis is in budding yeast, where the E3 ubiquitin ligase Psh1 mediates CENP-A^{Cse4} degradation to limit its incorporation into euchromatin (Hewawasam *et al.* 2010; Ranjitkar *et al.* 2010). Psh1 requires its association with the conserved FACT (Facilitates Chromatin Transcription/Transactions) complex to

doi: 10.1534/genetics.116.194027
Manuscript received July 20, 2016; accepted for publication October 26, 2016; published Early Online October 27, 2016.
Supplemental material is available online at http://www.genetics.org/cgi/content/full/genetics.116.194027/DC1.
[1]These authors contributed equally to this work.
[2]Corresponding author: Howard Hughes Medical Institute, Division of Basic Sciences, Fred Hutchinson Cancer Research Center, 1100 Fairview Ave. N., A2-168, PO Box 19024, Seattle, WA 98109. E-mail: sbiggins@fredhutch.org

bind to CENP-A^{Cse4} and mediate ubiquitylation, and a loss of this interaction results in CENP-A^{Cse4} mislocalization and cell death when CENP-A^{Cse4} is overexpressed (Deyter and Biggins 2014). FACT (consisting of the Spt16 and Pob3 proteins) influences many aspects of the dynamic nature of chromatin, and we previously proposed that its role in chromatin disassembly allows Psh1 to access mislocalized CENP-A^{Cse4} for ubiquitylation (Deyter and Biggins 2014). Proline isomerization is also important for CENP-A^{Cse4} degradation because it is impaired in *fpr3* and *fpr4* proline isomerase mutants (Ohkuni *et al.* 2014). CENP-A^{Cse4} has several proline residues that may require isomerization to promote an interaction with Psh1 (Ohkuni *et al.* 2014). Although CENP-A stably associates with histone H4 in CENP-A/H4 dimers and tetramers, the contribution of histone H4 or other features of the centromeric nucleosome to CENP-A proteolysis is unknown (Sekulic *et al.* 2010; Dechassa *et al.* 2014).

Here, we report that the histone H4 residue R36 contributes to CENP-A^{Cse4} degradation. CENP-A^{Cse4} overexpression is toxic to H4-R36A mutants, and this lethality is unrelated to centromere dysfunction because kinetochore composition and chromosome segregation are normal in these cells. Instead, overexpressed CENP-A^{Cse4} is stabilized and enriched in the euchromatin in the H4-R36A mutant, indicating a role for histone H4 in preventing CENP-A^{Cse4} mislocalization. Consistent with this, the interaction between Psh1 and CENP-A^{Cse4} is decreased in the H4 mutant. In addition, Psh1 becomes enriched at 3′ ends of genes, similar to the mislocalization pattern of the FACT component Spt16 in H4-R36A mutant cells (Nguyen *et al.* 2013). The mislocalization of Psh1 to 3′ intergenic regions raises the possibility that it has reduced access to CENP-A^{Cse4} at promoters and intragenic regions, resulting in elevated CENP-A^{Cse4} levels in the euchromatin. Together, our data identify a role for histone H4 in promoting an interaction between Psh1 and CENP-A^{Cse4} to prevent the promiscuous incorporation of CENP-A^{Cse4} into euchromatin.

Materials and Methods

Yeast strain construction and microbial techniques

Microbial techniques and media were performed as described (Deyter and Biggins 2014). For all experiments involving induction of epitope-tagged *pGAL-CSE4*, budding yeast cells of the indicated strains were grown to log phase (OD 0.55–0.8, Bio-Rad SmartSpec 3000) in lactic acid media at 23° and induced for 2 hr with 2% galactose, unless otherwise indicated. Yeast strains were constructed using standard genetic techniques (Sherman *et al.* 1974; Rose *et al.* 1990). Epitope-tagged proteins were constructed using either a PCR integration technique or by the integration of plasmids after restriction digestion (Longtine *et al.* 1998). Specific plasmids and yeast strains used in this study are described in Supplemental Material, Table S1 and Table S2, respectively. A *pGAL-3Flag-CSE4*, *LEU2* 2-μm vector (pSB1730) was constructed by digesting vector YEplac181 with *Kpn*I and *Sac*I (Gietz and Sugino 1988). The vector was ligated with a *pGAL-3Flag-CSE4* fragment that was isolated by digesting pSB839 (Ranjitkar *et al.* 2010) with the same enzymes to create a 2-μm *LEU2* plasmid with *pGAL-3Flag-CSE4* (pSB1730).

Genetic screen of histone mutant library

A previously constructed budding yeast histone H4 library was used to screen for mutants that are sensitive to CENP-A^{Cse4} overexpression (Dai *et al.* 2008; Ng *et al.* 2013). Each H4 amino acid was singly changed to alanine by integrating plasmids from a Histone Mutant Library version 2.1 (HMLv2.1) that had been digested with *Bci*VI to target the *HHT2-HHF2* locus in a *hht1-hhf1*Δ background (Dai *et al.* 2008; Ng *et al.* 2013). For convenience in the initial screen, we used a previously constructed library in our lab that also contained an Ipl1-degron protein (Ng *et al.* 2013). However, the strains were grown under conditions that did not promote Ipl1 degradation. First, the H4 library was transformed in 96-well plate format with a high-copy plasmid expressing Myc-tagged CENP-A^{Cse4} under the galactose promoter [pSB830 (Collins *et al.* 2004)] and subsequently plated on selective medium containing glucose in 100 × 15-mm plates. After 5 days of growth at 23°, transformants were patched onto selective medium containing glucose and incubated at 23°. Replica plating was performed to analyze the growth of the transformed library on glucose *vs.* galactose-containing medium. Hits were selected as strains that grew at 23° on glucose but exhibited defective growth on galactose-containing medium. To eliminate histone mutants that are defective in galactose metabolism, positive hits were rescreened to compare their growth on galactose with a control vector [YEplac181 (Gietz and Sugino 1988)] with that of the *pGAL-Myc-CSE4* plasmid [pSB830 (Collins *et al.* 2004)]. Hits were also streaked onto selective medium containing glucose or galactose to confirm the replica plating results. This initial round of screening identified six histone H4 mutants that appeared to have defective growth when CENP-A^{Cse4} was overexpressed: H4-I34A, H4-R36A, H4-K44A, H4-Y51A, H4-T80A, and H4-D85A. Second, the six H4 mutants were obtained from the same initial H4 mutant library and were retransformed with YEplac181 (vector control), pSB830 (*Myc-CSE4* plasmid), and pSB1730 (*pGAL-3Flag-CSE4*, which expresses CENP-A^{Cse4} at higher levels compared to the *pGAL-Myc-CSE4* plasmid) to reanalyze their growth on galactose-containing medium. This approach eliminated three of the mutants, leaving H4-R36A, H4-K44A, and H4-Y51A for further testing. These three H4 mutants were then regenerated in an otherwise wild-type (WT) background, where both histone loci were replaced with the mutants in contrast to the parent strains that had a single *HHF1-HHT1* locus replaced in the presence of an *HHF2-HHT2* deletion. These strains were made for each histone mutant of interest by integrating plasmids from a Histone Mutant Library version 3.0 (HMLv3.0) (a kind gift from Junbiao Dai, Tsinghua University) that were digested with *Bci*VI to target the *HHT1-HHF1* locus. The plasmids that were used to make the histone mutants were sequenced to confirm the presence of the desired mutation.

They were subsequently crossed to strains with the histone mutant of interest at the *HHT2-HHF2* locus to obtain strains with replacements at both histone loci. Plate spot assays (with yeast transformed with YEplac181 or pSB1730) were used to analyze the growth of the mutants on glucose and galactose medium for the final three candidates. The plasmids used to make these strains are listed in Table S1.

PyMOL structures

Preparation of structural figures of the human CENP-A [PDBID 3AN2 (Tachiwana *et al.* 2011)] and yeast H3 [PDBID 1ID3 (White *et al.* 2001)] nucleosomes were performed using the PyMOL Molecular Graphics System (Schrodinger).

Protein and immunoprecipitation techniques

Protein extracts to analyze total CENP-A^{Cse4} levels were prepared as described (Minshull *et al.* 1996; Hildebrand and Biggins 2016). Immunoblots using chemiluminescence were performed as previously described (Minshull *et al.* 1996; Hildebrand and Biggins 2016). For all immunoblots, the antibody dilutions were as follows: mouse α-Pgk1 monoclonal antibodies (Invitrogen, Carlsbad, CA, catalog # 459250) at a 1:10,000 dilution were used as a loading control. Mouse α-Flag M2 monoclonal antibodies (Sigma [Sigma-Chemical], St. Louis, MO, catalog # F3165) were used at a 1:3000 dilution, mouse α-HA 12CA5 monoclonal antibodies (Roche, catalog # 1-583-816) were used at a 1:10,000 dilution, rabbit α-H2B polyclonal antibodies (Active Motif, catalog # 39237) were used at a 1:3000 dilution, and mouse α-Myc 9E10 monoclonal antibodies were used at a 1:10,000 dilution (Covance, catalog # MMS-150R). Rabbit α-Spc105 antibodies were used at a 1:1000 dilution (Akiyoshi *et al.* 2010). Rabbit α-Ctf19 antibodies (a generous gift from Arshad Desai) were used at a 1:15,000 dilution. Quantitative immunoblots were carried out according to (Ng *et al.* 2013) with the modification of using 4% nonfat milk in PBS as the blocking agent for the α-Cse4 immunoblot. Briefly, IRDye anti-mouse and anti-rabbit secondary antibodies from LI-COR were used at a 1:5000 dilution. The immunoblots were imaged on a LI-COR imaging system, and the protein levels were quantified using Image Studio Lite.

Kinetochore purifications were performed from 50 ml cultures as previously described (Akiyoshi *et al.* 2010). For experiments analyzing ubiquitin conjugates of Cse4, NEM (*N*-ethylmaleimide) was added to the lysis and wash buffers to a final concentration of 5 mM (Deyter and Biggins 2014). Immunoprecipitates were separated by SDS-PAGE and analyzed by immunoblotting. Co-immunoprecipitation experiments were performed as previously described for Psh1-Myc and Spt16-Flag strains using protein G dynabeads conjugated with α-Myc (A-14, SC-789) and separated on a SDS-PAGE gel (Deyter and Biggins 2014).

Chromatin fractionation

Chromatin fractionation assays were performed as described, followed by analysis on immunoblots (Deyter and Biggins 2014). α-PGK1 was used as a marker and loading control for the soluble fraction, and α-H2B was used as a marker and loading control for the chromatin fraction (Deyter and Biggins 2014).

CENP-A^{Cse4} stability assays

CENP-A^{Cse4} stability assays were performed as in Deyter and Biggins (2014). Briefly, cells were grown in YEP + lactic acid until midlog phase, followed by a 2-hr 3Flag-Cse4 induction with 2% galactose. Glucose was added to a final concentration of 2% to further inhibit 3Flag-Cse4 transcription, and cycloheximide was added to a final concentration of 50 μg/ml. Time point 0 was taken immediately, followed by sample collection at the indicated time points. Extracts were prepared and analyzed as described (Minshull *et al.* 1996).

Chromosome segregation assay

Analysis of GFP-LacI was performed as described (Straight *et al.* 1996; Biggins *et al.* 1999). The lacO array was integrated at the *TRP1* locus, ~12.5 kb from *CEN4*.

Chromatin immunoprecipitation (ChIP)

ChIP was performed from 50 ml asynchronous yeast cultures with 1% formaldehyde to mediate cross-linking followed by sonication to fragment DNA, as previously described (Ng *et al.* 2009). α-Flag M2 antibodies conjugated to protein G dynabeads were used for both Flag-Cse4 and Psh1-Flag ChIPs. Quantitative polymerase chain reaction (qPCR) was performed as previously described (Hildebrand and Biggins 2016), on an Applied Biosystems (Foster City, CA) QuantStudio 5 qPCR machine. Oligonucleotide sequences are available in Table S3. Graphpad Prism 7 was used for two-way ANOVA with Tukey's multiple comparison tests to analyze Psh1 or CENP-A^{Cse4} enrichment, and to calculate Spearman's correlation coefficient for the Psh1 *vs.* CENP-A^{Cse4} data in the H4-R36A strain. Normalized ChIP signal for Psh1-Flag and Flag-Cse4 ChIPs was calculated as the mean of the ratio of the % Input for each strain relative to % Input for the WT *PSH1-Flag* or *pGAL-Flag-CSE4* strain, respectively, for three biological replicates.

PSH1 and CSE4 gene expression analysis

Gene expression of *PSH1* and *CSE4* in H4-R36A compared to WT cells was determined using published microarray data (Jung *et al.* 2015). The microarray data were accessed using the NCBI GEO accession viewer (GSE29059). A .txt file containing the log2 ratio of each gene in each histone mutant compared to WT was downloaded from this record (GSE29059_log2_mut_wt_ratio.txt.gz). This was imported into Microsoft Excel, and the log2 ratio for the H4-R36A mutant compared to the WT cells was looked up using the Microsoft Excel search function for *CSE4* (YKL049C, log2 H4-R36A *vs.* WT = 0.94562094) and *PSH1* (YOL054W, log2 H4-R36A *vs.* WT = 0.15504214). The paper that published the microarray data used a cutoff

of > 1.5-fold up- or downregulation to determine which genes were differentially regulated, and both *CSE4* and *PSH1* have < 1.5-fold change compared to WT (Jung *et al.* 2015).

Reagent and data availability

All strains and plasmids are available upon request. Table S1 describes the plasmids used to construct yeast strains, Table S2 lists the genotypes of all yeast strains, and Table S3 reports all oligonucleotide sequences used in this study.

Results

H4-R36A mutant cells are sensitive to CENP-A^{Cse4} overexpression

Because CENP-A^{Cse4} proline residues influence its degradation, we hypothesized that additional features of the CENP-A^{Cse4} nucleosome might be important for CENP-A^{Cse4} proteolysis (Ohkuni *et al.* 2014). CENP-A^{Cse4} binds with high affinity to histone H4 before and after deposition on DNA, so we asked whether histone H4 residues are important for CENP-A^{Cse4} degradation. To do this, we took advantage of the fact that mutants defective in CENP-A^{Cse4} degradation are sensitive to CENP-A^{Cse4} overexpression (Hewawasam *et al.* 2010; Ranjitkar *et al.* 2010). We used a previously constructed library of budding yeast histone H4 mutants, where each amino acid was changed to alanine, to screen for mutants that are intolerant to CENP-A^{Cse4} overexpression (Dai *et al.* 2008; Ng *et al.* 2013). We transformed the H4 library with a high-copy plasmid expressing N-terminally Myc-tagged CENP-A^{Cse4} under the galactose promoter and analyzed the growth of the cells on glucose- *vs.* galactose-containing medium. After subsequent rescreening (see *Materials and Methods*), only one histone H4 mutant, H4-R36A, exhibited significant lethality when CENP-A^{Cse4} was overproduced (Figure 1A and Figure S1A). Since arginine residues are subject to methylation in budding yeast, we created additional amino acid substitutions at H4 position 36 to test whether a post-translational modification might be involved (Rando and Winston 2012). We replaced R36 with a similarly basic residue lysine (R36K) that would inhibit methylation by an arginine methyltransferase. The growth of H4-R36K cells was similar to that of WT cells when CENP-A^{Cse4} was overexpressed, indicating that methylation is not involved. We also replaced H4-R36 with glutamic acid (R36E) to generate a negative charge and found it was nearly as sensitive to increased CENP-A^{Cse4} levels as H4-R36A cells (Figure 1A and Figure S1A). Together, these data indicate that a basic residue at position 36 in histone H4, but not post-translational modification of the amino acid, is required to prevent sensitivity to CENP-A^{Cse4} overexpression. Also, mutation of the neighboring H4-R35 residue did not cause sensitivity to CENP-A^{Cse4} (Figure 1B and Figure S1B), indicating a specific role for H4-R36 in protecting cells from CENP-A^{Cse4}-induced lethality. A notable feature of H4-R36 is that it is the only residue in the α-1 helix of H4 whose side chain interacts with nucleosomal DNA near the entry/exit site in canonical H3 nucleosomes and in octameric human CENP-A nucleosomes (Figure 1C) (Luger *et al.* 1997; Tachiwana *et al.* 2011). H4-R36 is also located in a region near to the CENP-A targeting domain (CATD) in the human CENP-A nucleosome, which is required for Psh1 recognition of CENP-A^{Cse4} (Figure 1D) (Ranjitkar *et al.* 2010; Tachiwana *et al.* 2011). These data suggest that the interaction between H4-R36 and DNA contributes to its function in shielding cells from the potentially lethal consequences of CENP-A^{Cse4} overexpression.

Kinetochores are functional in H4-R36A cells overexpressing CENP-A^{Cse4}

Since CENP-A^{Cse4} is essential for chromosome segregation, we asked if CENP-A^{Cse4} overexpression in H4-R36A cells altered kinetochore composition or function (Stoler *et al.* 1995). There is a precedent for H4 influencing chromosome segregation, since the *hhf1-20* mutation (conferring a H4-T82I/A89V substitution) that weakens the interface between H4 and DNA causes chromosome missegregation, as do other H4 mutations that were more recently identified (Smith *et al.* 1996; Kawashima *et al.* 2011; Ng *et al.* 2013). However, H4-R36A mutants have not been identified in any of these chromosome segregation screens and H4-R36A mutant cells do not show sensitivity to mitotic spindle poisons (Dai *et al.* 2008). We confirmed that the growth of H4-R36A cells was not affected by benomyl, a microtubule-destabilizing drug that inhibits the growth of kinetochore mutants and spindle assembly checkpoint mutants such as *mad1*Δ (Figure 2A and Figure S1C). We also tested whether CENP-A^{Cse4} still localizes to the centromere by performing ChIP followed by qPCR and detected similar levels of CENP-A^{Cse4} at *CEN4* in WT and H4-R36A cells overexpressing CENP-A^{Cse4} (Figure 2B).

We next analyzed the integrity of kinetochores by purification of the Dsn1 kinetochore protein, a method we previously developed to isolate native kinetochore particles (Akiyoshi *et al.* 2010). We immunoprecipitated Dsn1-3HA from WT and H4-R36A cells in the presence or absence of CENP-A^{Cse4} overexpression (Figure 2C). The levels of copurifying Ctf19 and Spc105, representative components of the inner and outer kinetochore, respectively, were similar to those of kinetochores isolated from WT and H4-R36A cells (Figure 2C). These data suggest that the overall kinetochore composition is not affected. To assess kinetochore function, we monitored chromosome segregation in H4-R36A cells that also carried a *mad1*Δ to inactivate the spindle assembly checkpoint and ensure similar cell cycle progression for all strains (Hardwick and Murray 1995). Cells containing a fluorescently marked chromosome IV were analyzed for segregation to opposite poles at anaphase (Straight *et al.* 1996). There was no significant difference in chromosome segregation between cells overexpressing CENP-A^{Cse4} in the presence or absence of the H4-R36A mutation (Figure 2D), indicating that the H4-R36 mutation

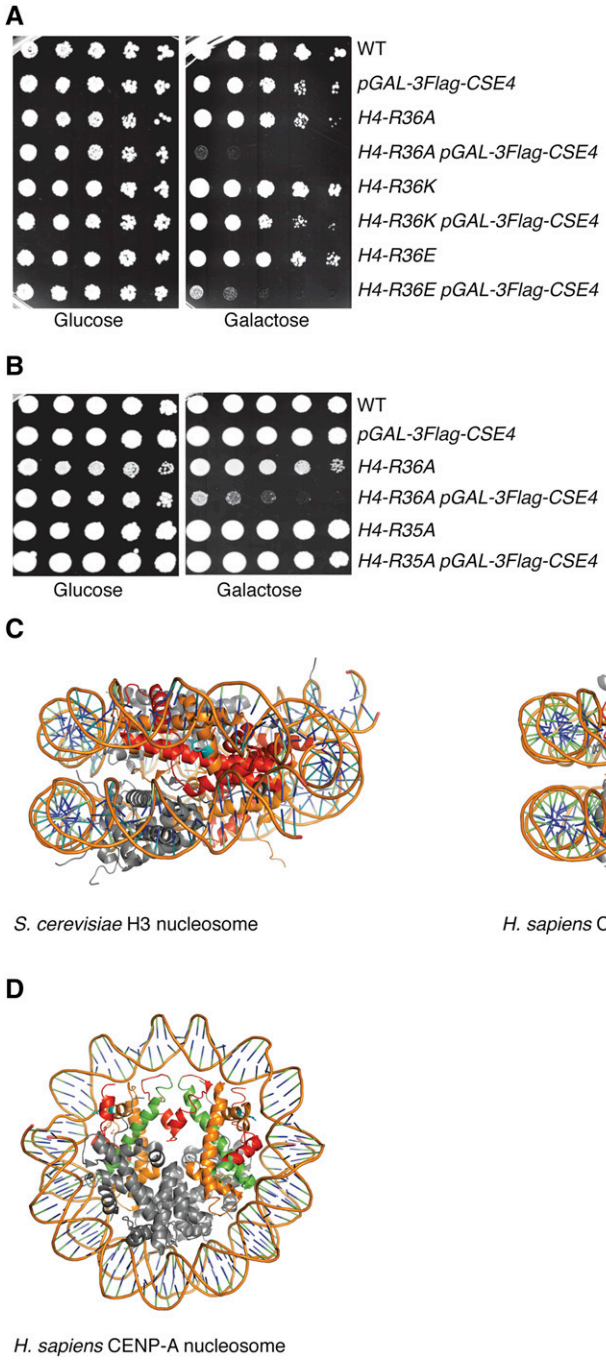

Figure 1 CENP-A^{Cse4} overexpression is lethal to H4-R36A cells. (A) Fivefold serial dilutions of the indicated strains [WT (SBY13389), *pGAL-3Flag-CSE4* (SBY13390), *H4-R36A* (SBY13391), *H4-R36A pGAL-3Flag-CSE4* (SBY13392), *H4-R36K* (SBY13393), *H4-R36K pGAL-3Flag-CSE4* (SBY13394), *H4-R36E* (SBY13395), and *H4-R36E pGAL-3Flag-CSE4* (SBY13396)] were plated on glucose or galactose media at 23°. (B) Fivefold dilutions of the indicated strains [WT (SBY9401), *pGAL-3Flag-CSE4* (SBY10025), *H4-R36A* (SBY9365), *H4-R36A pGAL-3Flag-CSE4* (SBY9397), *H4-R35A* (SBY10510), and *H4-R35A pGAL-3Flag-CSE4* (SBY13407)] were plated on glucose or galactose media at 23°. (C) Side views of crystal structures of the *S. cerevisiae* nucleosome containing histone H3 (left) and the *Homo sapiens* nucleosome containing CENP-A (right). Histone H4 (orange) residue R36 (cyan) makes side-chain interactions with nucleosomal DNA. Red: histone H3 (left) or CENP-A (right). (D) Top view of the crystal structure of the *H. sapiens* nucleosome containing CENP-A as in (C), with the CATD indicated (green). WT, wild-type.

does not significantly alter kinetochore composition or function.

Cells with reduced H3 levels are not sensitive to CENP-A^{Cse4} overexpression

The cellular levels of canonical H3 and CENP-A^{Cse4} are tightly regulated, and defects in H3 chromatin assembly can lead to CENP-A^{Cse4} incorporation (Sharp *et al.* 2002; Collins *et al.* 2004; Singh *et al.* 2009; Hewawasam *et al.* 2010; Ranjitkar *et al.* 2010; da Rosa *et al.* 2011; Eriksson *et al.* 2012; Kurat *et al.* 2014). Interestingly, H4-R36A is one of several histone mutants that have decreased H3 occupancy at highly transcribed genes (Hainer and Martens 2011). Therefore, we hypothesized that the sensitivity of H4-R36A cells to CENP-A^{Cse4} levels may be due to "gap-filling" in which defects in H3 chromatin occupancy provide nucleosome-depleted genomic regions that promote CENP-A^{Cse4} incorporation. If this were true, other histone mutants that are defective in H3 occupancy should also be sensitive to increased CENP-A^{Cse4} levels. To test this, we analyzed the growth of three other histone mutants in this class (H3-V46A, H3-R49A, and H4-I46A) when CENP-A^{Cse4} was overexpressed (Figure 3A and Figure S2A) (Hainer and Martens 2011). H3-V46A and H3-R49A cells exhibited a slight sensitivity to increased CENP-A^{Cse4}

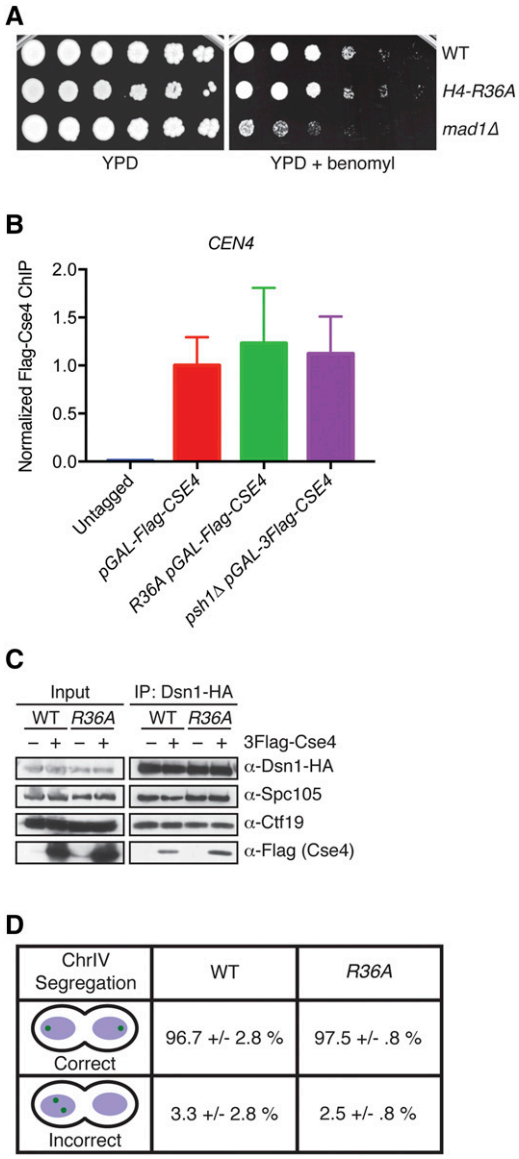

Figure 2 The overproduction of CENP-A^{Cse4} in the H4-R36A mutant does not perturb chromosome segregation. (A) WT (SBY9401), *H4-R36A* (SBY9979), and *mad1*Δ (SBY3256) cells were serially diluted five-fold and plated on YPD (left) or YPD + benomyl (right) medium and incubated at 23°. (B) 3Flag-Cse4 ChIP in WT (SBY16469), *H4-R36A* (SBY13812), and *psh1*Δ (SBY11189) cells with *pGAL-3Flag-CSE4* overexpression. An untagged strain (SBY3) was used as a negative control. qPCR for the *CEN4* locus (using primers SB3061 + SB3062) was performed. Normalized Flag-Cse4 ChIP is the ratio of the % Input in each strain relative to the % Input in the *pGAL-3Flag-CSE4* strain. Mean Flag-Cse4 ChIP enrichment ± 1 SE of the mean (SEM) for three biological replicates is shown. (C) Anti-HA-conjugated beads were used to immunoprecipitate kinetochores via Dsn1-3HA from WT (SBY10450) or *H4-R36A* (SBY10453) cells containing *pGAL-3Flag-CSE4* in the presence (+) or absence (−) of galactose. The levels of Spc105 and Ctf19 were analyzed by immunoblotting with antibodies raised against the respective proteins. Immunoblotting with α-HA antibodies revealed the levels of Dsn1-3HA in the immunoprecipitates while α-Flag antibodies detected the incorporation of overexpressed 3Flag-Cse4. (D) Asynchronous cultures of WT (SBY10494) or *H4-R36A* (SBY10391) cells with *mad1*Δ and expressing *pGAL-3Flag-CSE4* were grown in galactose for 4 hr and chromosome IV segregation was monitored in anaphase cells (defined by cells with DNA masses at opposite poles). At least 100 cells were counted for each strain from two independent replicates. Percent correct or incorrect segregation ± 1 SD is shown. ChIP, chromatin immunoprecipitation; Chr, chromosome; WT, wild-type.

levels, while H4-I46A cell growth was unaffected by CENP-A^{Cse4} overproduction. Notably, the H4-I46A mutant has a reduction in H3 chromatin assembly that is comparable to R36A cells, strongly suggesting that the lethality of CENP-A^{Cse4} overexpression in H4-R36A cells is not related to gap-filling. As an additional test of this model, we directly reduced H3 levels. H3 and H4 are transcribed from two loci, *HHT1-HHF1* and *HHT2-HHF2*. The major locus is *HHT2-HHF2*, and deleting this locus decreases the soluble pools of histones H3 and H4 (Liang *et al.* 2012). Therefore, we analyzed the growth of *hht2-hhf2*Δ cells when CENP-A^{Cse4} was overexpressed (Figure 3B and Figure S2B) and found no growth defect, indicating that reduced H3 levels do not sensitize cells to CENP-A^{Cse4} incorporation. Additionally, H4-R36A *hht2-hhf2*Δ cells did not show a more severe phenotype with CENP-A^{Cse4} overexpression compared to H4-R36A cells. Altogether, these data suggest that altered H3 levels likely play a minimal role in the sensitivity of H4-R36A cells to increased CENP-A^{Cse4} protein.

CENP-A^{Cse4} is mislocalized in H4-R36A cells

Because the sensitivity of cells to CENP-A^{Cse4} overexpression correlates with the level of CENP-A^{Cse4} misincorporation into euchromatin, we asked whether CENP-A^{Cse4} localizes to euchromatin in H4-R36A cells (Hewawasam *et al.* 2010; Ranjitkar *et al.* 2010; Hildebrand and Biggins 2016). To test this, we compared the levels of overexpressed CENP-A^{Cse4} in soluble and chromatin fractions from WT, H4-R36A, and *psh1*Δ cells. As we previously showed, the levels of CENP-A^{Cse4} are higher in *psh1*Δ than WT since CENP-A^{Cse4} is stabilized (Ranjitkar *et al.* 2010) (Figure 4A). Similarly, CENP-A^{Cse4} levels are also higher in H4-R36A cells compared to WT cells, and it is enriched in the chromatin fraction of H4-R36A cells, although to a lesser extent than *psh1*Δ cells (Figure 4A and Figure S3).

The interaction between Psh1 and CENP-A^{Cse4} is altered in the H4-R36A mutant

The increased CENP-A^{Cse4} protein levels in H4-R36A cells suggested a defect in CENP-A^{Cse4} proteolysis because there are no changes in *PSH1* or *CSE4* transcription in these cells [see *Materials and Methods* and Jung *et al.* (2015)]. To determine if CENP-A^{Cse4} degradation is impaired in H4-R36A cells, we monitored CENP-A^{Cse4} protein levels after transient overexpression followed by translational repression with cycloheximide. CENP-A^{Cse4} was partially stabilized in H4-R36A cells compared to WT cells (Figure 4B). To determine whether this is a result of a reduction in ubiquitin-mediated proteolysis, we analyzed the level of CENP-A^{Cse4} ubiquitin conjugates in WT, *psh1*Δ, and H4-R36A cells. As expected,

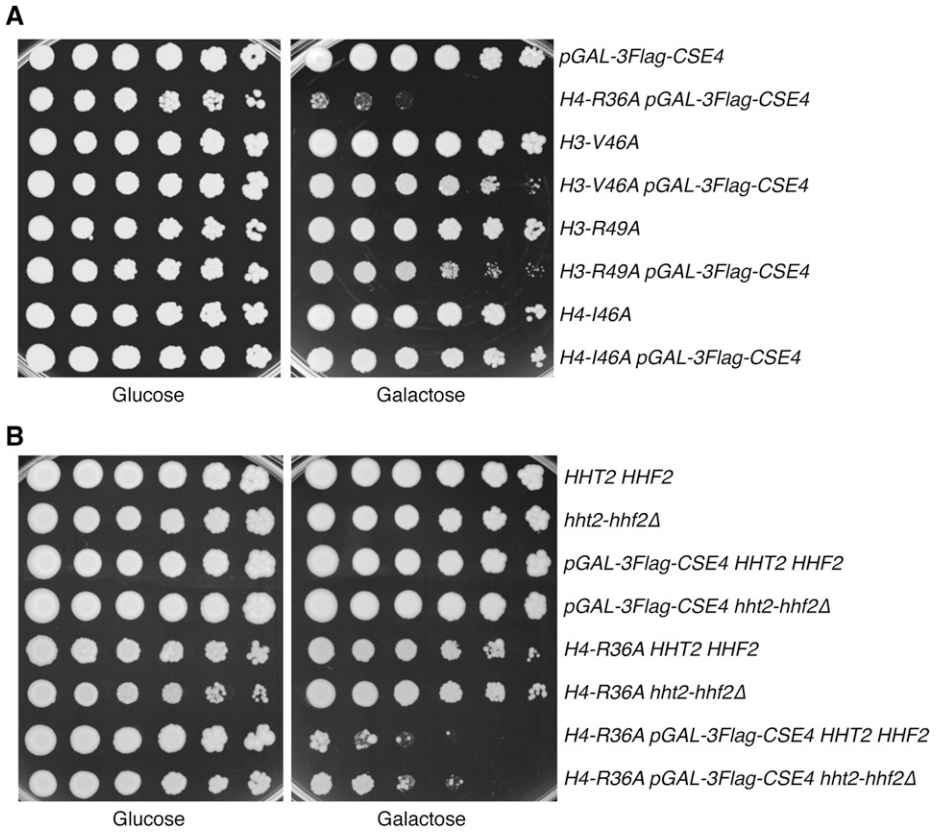

Figure 3 The sensitivity of H4-R36A cells to CENP-A^{Cse4} overexpression is not due to H3 depletion. (A) Fivefold serial dilutions of the indicated strains [*pGAL-3Flag-CSE4* (SBY10025), *H4-R36A pGAL-3Flag-CSE4* (SBY9397), *H3-V46A* (SBY10392), *H3-V46A pGAL-3Flag-CSE4* (SBY10511), *H3-R49A* (SBY10393), *H3-R39A pGAL-3Flag-CSE4* (SBY10512), *H4-I46A* (SBY10394), and *H4-I46A pGAL-3Flag-CSE4* (SBY10513)] were plated on glucose or galactose media at 23°. (B) Fivefold dilutions of the indicated strains [*HHT2-HHF2* (SBY9401), *hht2-hhf2Δ* (SBY10730), *pGAL-3Flag-CSE4 HHT2-HHF2* (SBY10025), *pGAL-3Flag-CSE4 hht2-hhf2Δ* (SBY10734), *H4-R36A HHT2-HHF2* (SBY9365), *H4-R36A hht2-hhf2Δ* (SBY10778), *H4-R36A pGAL-3Flag-CSE4 HHT2-HHF2* (SBY9397), and *H4-R36A pGAL-3Flag-CSE4 hht2-hhf2Δ* (SBY10782)] were plated on glucose or galactose media at 23°.

CENP-A^{Cse4} isolated from WT cells displayed several higher mobility species, most of which correspond to ubiquitin conjugates of CENP-A^{Cse4} (Figure 4, C and D). Consistent with previous work, ubiquitin conjugates of CENP-A^{Cse4} are decreased in *psh1*Δ cells (Hewawasam *et al.* 2010; Ranjitkar *et al.* 2010). The upper CENP-A^{Cse4} forms that are present in the *psh1*Δ cells correspond to SUMO conjugates that become detectable when ubiquitylation is reduced (Ranjitkar *et al.* 2010; Ohkuni *et al.* 2016) (Figure 4C and data not shown). CENP-A^{Cse4} isolated from H4-R36A cells showed lower levels of most ubiquitin conjugates and increased sumoylation compared to WT cells, consistent with its partial stabilization. Together, these results show that H4-R36A cells are partially defective in CENP-A^{Cse4} degradation and accumulate CENP-A^{Cse4} in euchromatin.

The increased stability of CENP-A^{Cse4} in H4-R36A cells suggested that the interaction between CENP-A^{Cse4} and Psh1 might be altered in the mutant. Indeed, the association between Psh1 and CENP-A^{Cse4} is reduced when Psh1 is immunoprecipitated from H4-R36A cells compared to WT cells (Figure 4E). The CENP-A^{Cse4}/Psh1 ratio ± 1 SE of the mean (SEM) *vs.* WT for H4-R36A cells was 0.5 ± 0.03. Consistent with our data suggesting that residue 36 of H4 needs to be basic to protect cells from lethality when CENP-A^{Cse4} is overproduced (Figure 1A), the Psh1-CENP-A^{Cse4} interaction is retained in the H4-R36K mutant that restores the basic charge (Figure 4E). The CENP-A^{Cse4}/Psh1 ratio ± 1 SEM *vs.* WT for H4-R36K cells was 3.0 ± 0.6. Taken together, these results suggest that the defects in CENP-A^{Cse4} proteolysis are likely due to a decreased interaction between Psh1 and CENP-A^{Cse4} in H4-R36A.

Psh1 is enriched at the 3′ ends of genes in H4-R36A cells

The altered Psh1-CENP-A^{Cse4} interaction could be due to a change in CENP-A^{Cse4} nucleosome structure that directly affects the binding of CENP-A^{Cse4} to Psh1, and/or it could be due to changes in the localization of Psh1 such that it is no longer available to bind to CENP-A^{Cse4} nucleosomes. Psh1 is present in both the soluble and chromatin fractions of cells; however, its euchromatic localization pattern has not been analyzed (Hewawasam *et al.* 2010; Ranjitkar *et al.* 2010). In addition, Psh1 is known to associate with FACT (Ranjitkar *et al.* 2010; Deyter and Biggins 2014), although their level of colocalization throughout the genome is unknown. The FACT complex exhibits an altered localization pattern in H4-R36A mutants and becomes enriched at the 3′ untranslated region (UTR) of highly transcribed genes (Nguyen *et al.* 2013). This phenotype is also shared with other histone mutants including H4-R31E and H3-L61W (Duina *et al.* 2007; Nguyen *et al.* 2013). These residues map to a distinct area of the nucleosome, and it was proposed that this nucleosomal region releases FACT from the end of transcribed units, although the exact mechanism or signal for the dissociation remains unclear (Duina *et al.* 2007; Nguyen *et al.* 2013).

Because Psh1 association with FACT is important for CENP-A^{Cse4} ubiquitylation and degradation (Deyter and

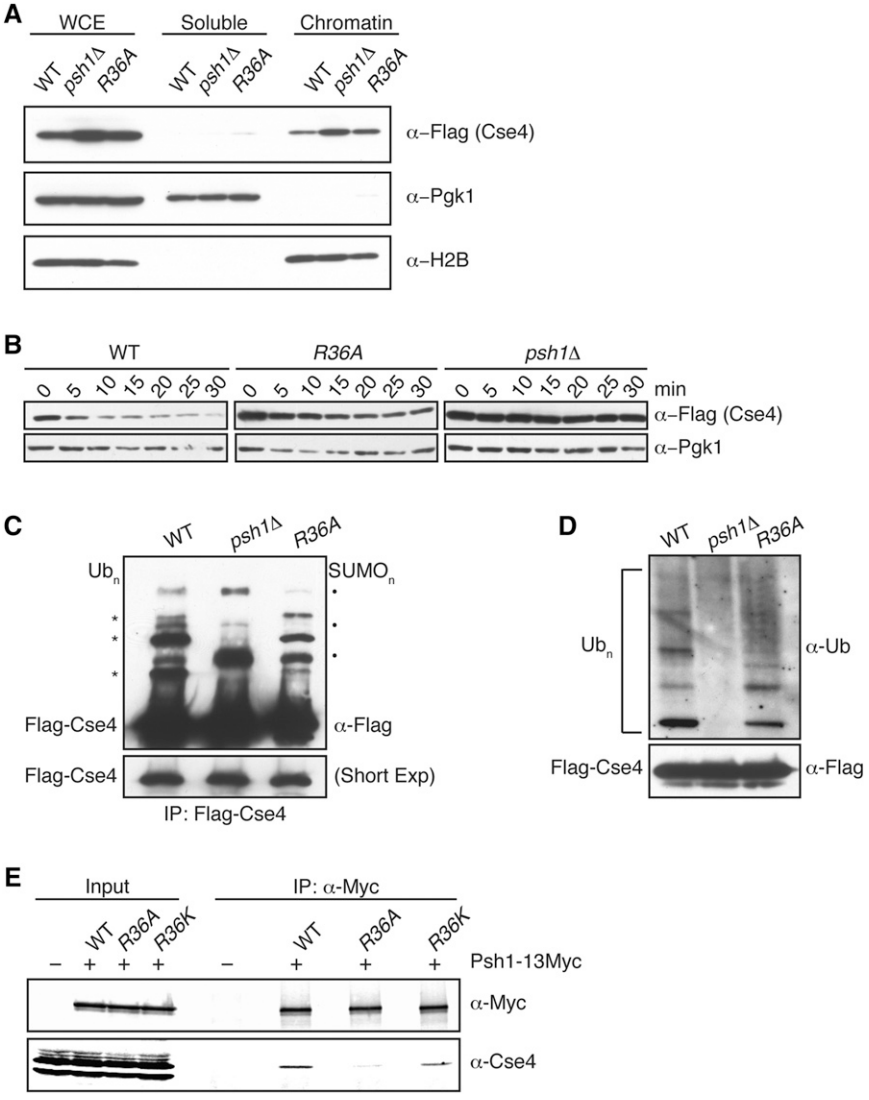

Figure 4 H4-R36A cells have defects in CENP-A^{Cse4} degradation. (A) WCE from WT (SBY10025), *psh1*Δ (SBY10590), and *H4-R36A* (SBY9397) cells expressing *pGAL-3Flag-CSE4* were fractionated into soluble and chromatin fractions. 3Flag-Cse4 levels were monitored in each fraction with α-Flag antibodies. Pgk1 and H2B are markers of the soluble and chromatin fractions, respectively. Note that a longer exposure of the blot for CENP-A^{Cse4} is included in Figure S3, which shows CENP-A^{Cse4} in the soluble fraction. (B) WT (SBY10025), *H4-R36A* (SBY9397), and *psh1*Δ (SBY10590) cells expressing *pGAL-3Flag-CSE4* were grown in galactose, protein synthesis was inhibited by cycloheximide addition at time zero, and lysates were monitored for 3Flag-Cse4 levels at the indicated time points with α-Flag antibodies. Pgk1 served as a loading control. (C) WT (SBY10025), *psh1*Δ (SBY10590), and *H4-R36A* (SBY9397) cells expressing *pGAL-3Flag-CSE4* were grown in galactose and 3Flag-Cse4 was immunoprecipitated with α-Flag antibodies. Unmodified 3Flag-Cse4 and its higher-mobility species (Ub$_n$) were detected on immunoblots by probing with α-Flag antibodies, these bands are marked on the left by asterisks. Note that SUMO conjugates appear on Cse4 in the absence of ubiquitylation (SUMO$_n$), these bands are marked on the right by solid dots (Ohkuni *et al.* 2016). The lower panel shows a shorter exposure of the immunoblot to display the levels of unmodified 3Flag-Cse4 in the immunoprecipitates and serves as a loading control. (D) An immunoblot probed with α-ubiquitin antibodies of the α-Flag immunoprecipitates isolated from the strains denoted in (C) reveals the ubiquitin conjugates of 3Flag-Cse4. The lower panel shows the levels of unmodified 3Flag-Cse4 by immunoblotting with α-Flag antibodies. (E) Psh1-13Myc was immunoprecipitated from WT (SBY15335), *H4-R36A* (SBY15624), and *H4-R36K* (SBY16468) cells, and immunoblots were probed with α-Myc and α-Cse4 antibodies. Cells expressing untagged Psh1 (SBY3) served as a control. The Cse4/Psh1 ratio ± 1 SEM was calculated *vs.* WT for *H4-R36A* (0.5 ± 0.03) and *H4-R36K* (3.0 ± 0.6) from three biological replicates. IP, immunoprecipitation; WCE, whole cell extract; WT, wild-type.

Biggins 2014), we analyzed Psh1 localization in WT *vs.* H4-R36A cells at the 5′, 3′, and coding regions of two highly transcribed genes, *ADH1* and *PMA1*. It was previously found that the Spt16 component of FACT is mislocalized to the 3′ UTRs of these genes in H4-R36A or H3-L61W mutant cells (Duina *et al.* 2007; Nguyen *et al.* 2013). We confirmed the enrichment of Spt16 to the 3′ UTRs of the *ADH1* and *PMA1* genes in the H4-R36A mutants in our strain background using ChIP-PCR (data not shown). Strikingly, ChIP-qPCR revealed that Psh1 also shows a strong enrichment at the 3′ UTRs of these genes in H4-R36A cells compared to WT, while the levels at the promoter and gene regions were similar to WT cells (Figure 5, A–D). The H4-R36K mutant, which rescues the Psh1-CENP-A^{Cse4} interaction, also restores the WT Psh1 localization pattern (Figure 5, C and D). Together, these data suggest that altered Psh1 localization could contribute to the CENP-A^{Cse4} stability phenotype in H4-R36A mutant cells.

CENP-A^{Cse4} mislocalization is negatively correlated with Psh1 enrichment in H4-R36A cells

We previously discovered that overexpressed CENP-A^{Cse4} is mislocalized to nucleosomes in both tandem and divergent intergenic regions in the absence of Psh1 (Hildebrand and Biggins 2016). To test whether this is also true in the H4-R36A mutant cells, we performed ChIP-qPCR on overexpressed CENP-A^{Cse4} from WT, H4-R36A, and *psh1*Δ cells, and analyzed CENP-A^{Cse4} enrichment at the *ADH1* and *PMA1* promoters, genes, and 3′ regions compared to the WT *pGAL-3Flag-CSE4* strain. For both genes, overexpressed CENP-A^{Cse4} is enriched in the promoter and coding regions in

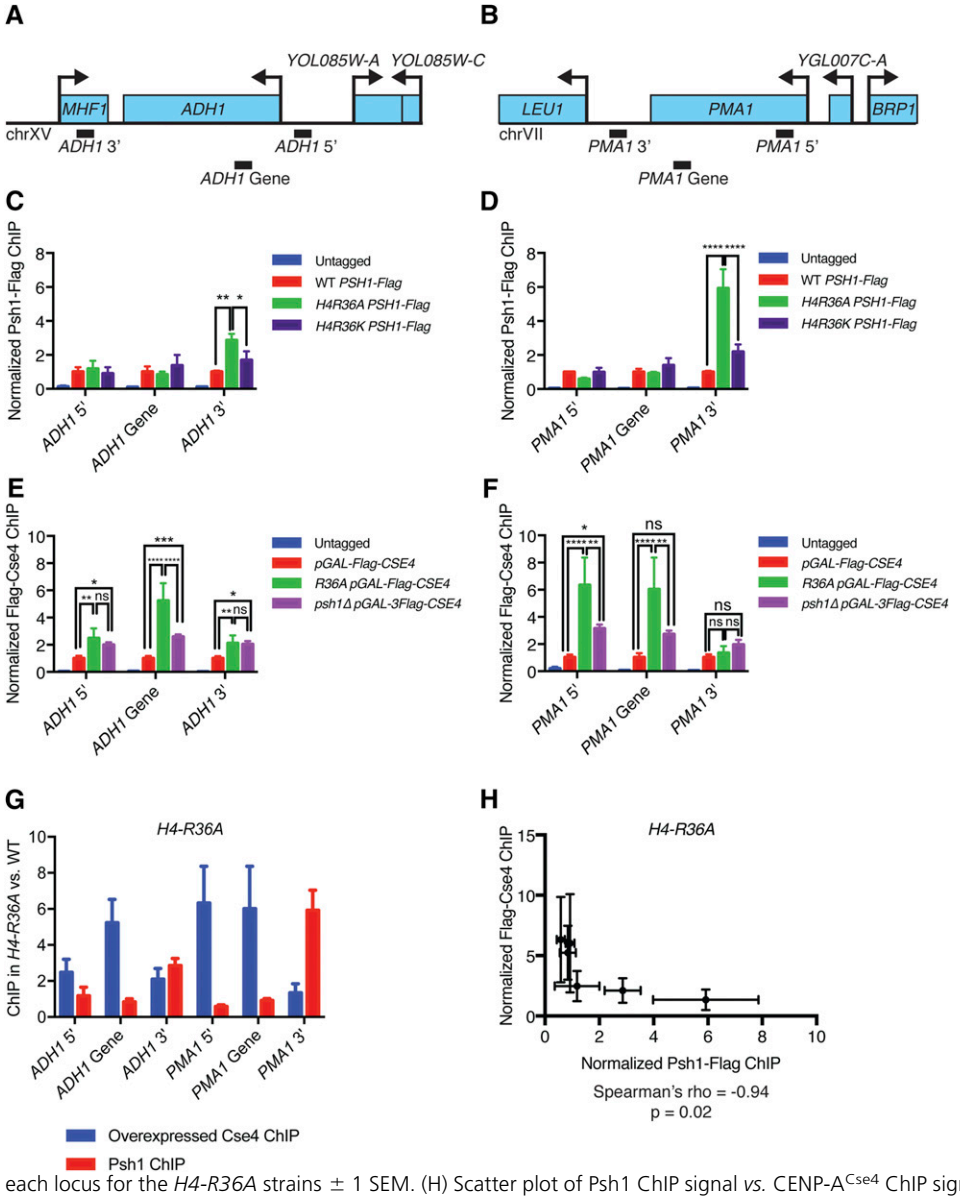

Figure 5 Psh1 and CENP-A^{Cse4} are mislocalized in the H4-R36A mutant cells. (A) Diagram of the *ADH1* genomic locus showing regions amplified by 5′, 3′, and intragenic primer sets (not to scale). (B) Diagram of the *PMA1* genomic locus showing regions amplified by the 5′, 3′, and intragenic primer sets (not to scale). (C) Psh1-3Flag ChIP from WT (SBY13723), *H4-R36A* (SBY13725), and *H4-R36K* (SBY16594) cells. Cells expressing untagged Psh1 (SBY3) were used as controls. qPCR was performed for the primer sets shown in (A), *ADH1* 5′ (SB5059 and SB5060), *ADH1* gene (SB4470 and SB4471), and *ADH1* 3′ (SB4472 and SB4473). Normalized Psh1-Flag ChIP is the ratio of the % Input in each strain relative to the % Input in the WT *PSH1-Flag* strain. Mean Psh1-Flag ChIP enrichment ± 1 SEM from three biological replicates is shown. Results from two-way ANOVA with Tukey's multiple comparisons test are shown. * $P < 0.05$, ** $P \leq 0.01$, *** $P \leq 0.001$, **** $P \leq 0.0001$. (D) Psh1-Flag ChIP as in (C), with PCR primers as shown in (B) for *PMA1* 5′ (SB5029 and SB5030), *PMA1* gene (SB4076 and SB4077), and *PMA1* 3′ (SB5027 and SB5028). (E) ChIP of overexpressed Flag-Cse4 from WT (SBY16469), *H4-R36A* (SBY13812), and *psh1*Δ (SBY11189) strains. Cells expressing untagged CENP-A^{Cse4} were used as a control (SBY3). PCR primers at the *ADH1* locus were used as in (C). qPCR was performed, normalized Flag-Cse4 ChIP is the ratio of the % Input in each strain relative to the % Input in the *pGAL-3Flag-CSE4* strain. Mean Flag-Cse4 ChIP enrichment ± 1 SEM from three biological replicates is shown. (F) Flag-Cse4 ChIP as in (E) for *PMA1* primers as in (D). (G) Bar plot of the average CENP-A^{Cse4} (blue) or Psh1 (red) ChIP signal at each locus for the *H4-R36A* strains ± 1 SEM. (H) Scatter plot of Psh1 ChIP signal *vs.* CENP-A^{Cse4} ChIP signal at each locus as in (G) (average ± 1 SD) in the *H4-R36A* strains. Spearman's correlation coefficient was calculated from these data ($\rho = -0.94$, $P = 0.02$). ChIP, chromatin immunoprecipitation; chr, chromosome; qPCR, quantitative PCR; WT, wild-type; ns, not significant.

H4-R36A cells compared to WT and *psh1*Δ mutant cells (Figure 5, E and F). In contrast, the level of CENP-A^{Cse4} mislocalization at the 3′ ends of these genes is either much lower (at the *ADH1* 3′ end) or not enriched at all (at the *PMA1* 3′ end). Strikingly, correlation analysis of Psh1 and CENP-A^{Cse4} localization in the H4-R36A strain reveals a significant negative correlation (Spearman's $\rho = -0.9429$, $P = 0.0167$) (Figure 5, G and H). This finding is consistent with the possibility that the local enrichment of Psh1 mediates the ubiquitylation and degradation of CENP-A^{Cse4} at specific regions.

Discussion

In this study, we performed the first systematic screen to identify mutations in H4 that affect the regulation of the histone variant CENP-A^{Cse4}. The H4 mutant R36A exhibited the strongest sensitivity to CENP-A^{Cse4} overexpression of those analyzed. Our genetic and biochemical analyses support a model whereby a positive charge at this residue is required for CENP-A^{Cse4} regulation by ensuring that the Psh1 ubiquitin ligase interacts with CENP-A^{Cse4}.

The H4-R36A cells overexpressing CENP-A^{Cse4} are most likely inviable due to mislocalization of the centromeric histone variant to the euchromatin. We previously determined that CENP-A^{Cse4} overexpression is lethal in cells lacking Psh1 due to ectopic localization of the centromeric histone variant, and here we found that Psh1 exhibits reduced binding to its substrate in the H4-R36A mutant cells (Ranjitkar *et al.* 2010; Deyter and Biggins 2014). Consistent with this, there was an increase in CENP-A^{Cse4} stability and a reduction in its

ubiquitylated forms in the H4-R36A mutant cells. Since H4-R36A cells have transcriptional defects as well as decreased nucleosome occupancy at transcribed genes, it is possible that increased transcriptional stress in the presence of mislocalized CENP-A^{Cse4} contributes to cell death (Dai *et al.* 2008; Hainer and Martens 2011; Nguyen *et al.* 2013; Jung *et al.* 2015; Hildebrand and Biggins 2016). However, the lethality induced by CENP-A^{Cse4} overexpression is rescued in the H4-R36K mutant, which restores the interaction between Psh1 and CENP-A^{Cse4} but not all of the other H4-R36A phenotypes (Dai *et al.* 2008). Together, these data strongly suggest that the reduced interaction between Psh1 and CENP-A^{Cse4} is related to the cell death caused by CENP-A^{Cse4} overexpression.

The reduced Psh1-CENP-A^{Cse4} interaction in the H4-R36A mutant cells could be due to a change in the nucleosome or (CENP-A^{Cse4}-H4)$_2$ tetramer structure that directly alters the binding site of Psh1 for CENP-A^{Cse4}. The CATD of CENP-A^{Cse4} is required for Psh1 binding and H4-R36 is not predicted to directly contact the CATD in an octameric nucleosome (Ranjitkar *et al.* 2010; Tachiwana *et al.* 2011). However, H4-R36 contacts the DNA near the DNA entry/exit site on the nucleosome and this region is close to the CATD (White *et al.* 2001; Tachiwana *et al.* 2011). Therefore, this residue may directly contribute to Psh1 recognition of the nucleosome and help distinguish nucleosome-bound *vs.* soluble CENP-A^{Cse4}.

The decreased binding between Psh1 and CENP-A^{Cse4} may also be due to an indirect mechanism related to altered localization of the ubiquitin ligase. We found that Psh1 becomes enriched at 3′ UTRs in H4-R36A cells at two loci. If this is a widespread phenomenon, it could explain the decreased Psh1-CENP-A^{Cse4} interaction, since Psh1 may be sequestered at 3′ UTRs. Consistent with this, there appears to be a negative correlation between the enrichment of Psh1 and CENP-A^{Cse4} in H4-R36A cells at these loci, raising the possibility that there is localized degradation of CENP-A^{Cse4} at the 3′ sites where Psh1 accumulates. In the future, ChIP-seq assays to determine the genome-wide mislocalization pattern of CENP-A^{Cse4} and Psh1 in H4-R36A cells may further elucidate the underlying mechanism.

It is unclear what mechanism underlies the Psh1 3′ UTR enrichment. This mislocalization pattern is similar to what has been seen for the FACT complex component Spt16 in H4-R36A cells (Nguyen *et al.* 2013). Since Psh1 binds to Spt16 and this interaction is essential for controlling CENP-A^{Cse4} localization *in vivo*, one possibility is that the mislocalization of FACT in H4-R36A cells leads to Psh1 enrichment at 3′ UTRs (Ranjitkar *et al.* 2010; Deyter and Biggins 2014). However, there are intragenic Spt16 suppressors that relieve its accumulation at the 3′ UTR in the H4-R36A mutant cells, but only some of them suppress the lethality of CENP-A^{Cse4} overexpression (data not shown) (Duina *et al.* 2007; Nguyen *et al.* 2013). Therefore, the underlying mechanism appears to be more complicated than just FACT mislocalization leading to the accumulation of Psh1 at 3′ UTR regions. Consistent with this, while both Psh1 and Spt16 are enriched at 3′ UTRs in H4-R36A cells, only Spt16 shows depletion at promoters and intragenic regions (Nguyen *et al.* 2013).

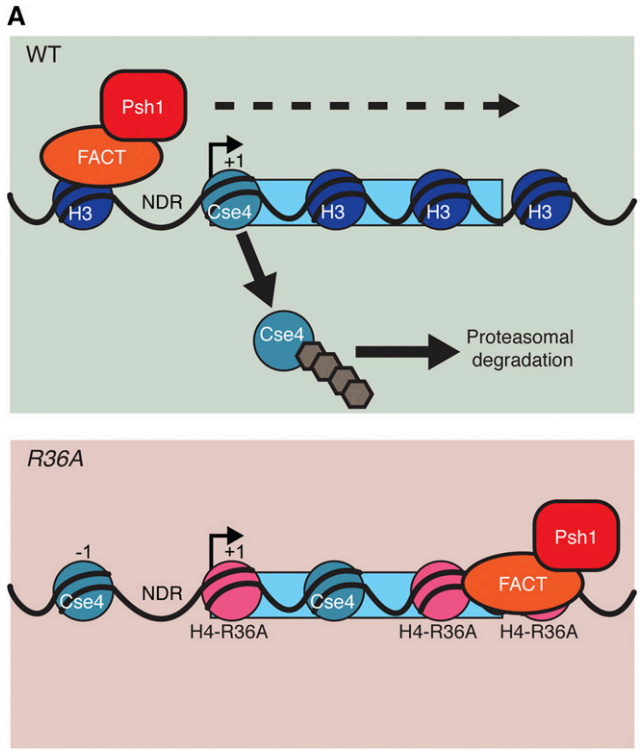

Figure 6 Model for control of CENP-A^{Cse4} localization via a dynamic Psh1-chromatin interaction. In WT cells containing canonical nucleosomes (dark blue), Psh1 (red) and FACT (orange) interact dynamically with genes during transcription (dynamic interaction is indicated by dashed arrow). This allows Psh1 to recognize mislocalized CENP-A^{Cse4} (teal) at 5′, intragenic, and 3′ regions and mediate its ubiquitylation (brown), leading to its proteasomal degradation. Psh1-mediated recognition and degradation enables the cells to control CENP-A^{Cse4} localization and to live when CENP-A^{Cse4} is overexpressed (green shaded box). When H4-R36 is mutated to alanine (pink), FACT and Psh1 lose their dynamic interaction with transcribed genes and are sequestered at 3′ UTRs, compromising the Psh1/CENP-A^{Cse4} interaction. CENP-A^{Cse4} that incorporates at 5′ or intragenic regions is not adequately ubiquitylated and is retained at ectopic sites, leading to cell death (red shaded box). WT, wild-type.

While the precise reason for the Psh1 mislocalization to 3′ ends of genes is not clear, it is correlated with altered CENP-A^{Cse4} localization. Therefore, we propose that Psh1 needs to dynamically associate with chromatin to regulate CENP-A^{Cse4} (Figure 6). This is consistent with our previous conclusion that Psh1 needs to be traveling with FACT and elongating RNA polymerases to recognize CENP-A^{Cse4} that is incorporated into nucleosomes (Deyter and Biggins 2014). By disrupting chromatin, FACT would allow Psh1 to access the CATD, which is normally buried in the core of the nucleosome. The position of H4-R36 near the nucleosome entry/exit site may facilitate the ability of FACT to disrupt nucleosome structure. When this residue is disrupted, it may alter Psh1 and FACT localization in a manner that impairs CENP-A^{Cse4} proteolysis, possibly by preventing the dynamic movement of FACT and Psh1 (Figure 6).

In summary, our work has identified another facet of the regulation of CENP-A^{Cse4} protein levels and localization. Histone H4 residue (R36) facilitates the Psh1-CENP-A^{Cse4} physical interaction, likely by allowing Psh1 and FACT to travel dynamically through genes during transcription to facilitate CENP-A^{Cse4} removal and degradation. Because it is essential to maintain the exclusive localization of the centromeric histone to prevent genomic instability and transcriptional misregulation (Hewawasam *et al.* 2010; Ranjitkar *et al.* 2010; Hildebrand and Biggins 2016), it will be important to further elucidate the precise nature of the interaction between Psh1 and the centromeric nucleosome, as well as the dynamics of Psh1 localization to chromatin in the future.

Acknowledgments

We thank Junbiao Dai for providing the plasmids required to generate the histone mutant strains, and Arshad Desai for sharing α-Ctf19 antibodies. We thank members of the Tsukiyama and Biggins laboratories for helpful discussions and advice and T. Tsukiyama and M. Basrai for critical reading of the manuscript. Research was funded by a National Institutes of Health grant Regulation of Centromeric Chromatin (R01 GM-078069) to S.B., an American Cancer Society fellowship to G.M.R.D., a National Institutes of Health Chromosome Metabolism and Cancer Training grant (T32CA009657), and a National Science Foundation Graduate Research Fellowship Program to E.M.H. S.B. is an Investigator of the Howard Hughes Medical Institute.

Literature Cited

Akiyoshi, B., K. K. Sarangapani, A. F. Powers, C. R. Nelson, S. L. Reichow *et al.*, 2010 Tension directly stabilizes reconstituted kinetochore-microtubule attachments. Nature 468: 576–579.

Amato, A., T. Schillaci, L. Lentini, and A. Di Leonardo, 2009 CENP-A overexpression promotes genome instability in pRb-depleted human cells. Mol. Cancer 8: 119.

Biggins, S., F. F. Severin, N. Bhalla, I. Sassoon, A. A. Hyman *et al.*, 1999 The conserved protein kinase Ipl1 regulates microtubule binding to kinetochores in budding yeast. Genes Dev. 13: 532–544.

Black, B. E., and D. W. Cleveland, 2011 Epigenetic centromere propagation and the nature of CENP-A nucleosomes. Cell 144: 471–479.

Collins, K. A., S. Furuyama, and S. Biggins, 2004 Proteolysis contributes to the exclusive centromere localization of the yeast Cse4/CENP-A histone H3 variant. Curr. Biol. 14: 1968–1972.

da Rosa, J. L., J. Holik, E. M. Green, O. J. Rando, and P. D. Kaufman, 2011 Overlapping regulation of CenH3 localization and histone H3 turnover by CAF-1 and HIR proteins in *Saccharomyces cerevisiae*. Genetics 187: 9–19.

Dai, J., E. M. Hyland, D. S. Yuan, H. Huang, J. S. Bader *et al.*, 2008 Probing nucleosome function: a highly versatile library of synthetic histone H3 and H4 mutants. Cell 134: 1066–1078.

Dechassa, M. L., K. Wyns, and K. Luger, 2014 Scm3 deposits a (Cse4–H4)2 tetramer onto DNA through a Cse4–H4 dimer intermediate. Nucleic Acids Res. 42: 5532–5542.

Deyter, G. M. R., and S. Biggins, 2014 The FACT complex interacts with the E3 ubiquitin ligase Psh1 to prevent ectopic localization of CENP-A. Genes Dev. 28: 1815–1826.

Duina, A. A., A. Rufiange, J. Bracey, J. Hall, A. Nourani *et al.*, 2007 Evidence that the localization of the elongation factor Spt16 across transcribed genes is dependent upon histone H3 integrity in *Saccharomyces cerevisiae*. Genetics 177: 101–112.

Eriksson, P. R., D. Ganguli, V. Nagarajavel, and D. J. Clark, 2012 Regulation of histone gene expression in budding yeast. Genetics 191: 7–20.

Gietz, R. D., and A. Sugino, 1988 New yeast-*Escherichia coli* shuttle vectors constructed with *in vitro* mutagenized yeast genes lacking six-base pair restriction sites. Gene 74: 527–534.

Gross, S., F. Catez, H. Masumoto, and P. Lomonte, 2012 Centromere architecture breakdown induced by the viral E3 ubiquitin ligase ICP0 protein of herpes simplex virus type 1. PLoS One 7: e44227.

Hainer, S. J., and J. A. Martens, 2011 Identification of histone mutants that are defective for transcription-coupled nucleosome occupancy. Mol. Cell. Biol. 31: 3557–3568.

Hardwick, K., and A. W. Murray, 1995 Mad1p, a phosphoprotein component of the spindle assembly checkpoint in budding yeast. J. Cell Biol. 131: 709–720.

Heun, P., S. Erhardt, M. D. Blower, S. Weiss, A. D. Skora *et al.*, 2006 Mislocalization of the *Drosophila* centromere-specific histone CID promotes formation of functional ectopic kinetochores. Dev. Cell 10: 303–315.

Hewawasam, G., M. Shivaraju, M. Mattingly, S. Venkatesh, S. Martin-Brown *et al.*, 2010 Psh1 is an E3 ubiquitin ligase that targets the centromeric histone variant Cse4. Mol. Cell 40: 444–454.

Hildebrand, E. M., and S. Biggins, 2016 Regulation of budding yeast CENP-A levels prevents misincorporation at promoter nucleosomes and transcriptional defects. PLoS Genet. 12: e1005930.

Jung, I., J. Seo, H. S. Lee, L. W. Stanton, D. Kim *et al.*, 2015 Global mapping of the regulatory interactions of histone residues. FEBS Lett. 589: 4061–4070.

Kawashima, S., Y. Nakabayashi, K. Matsubara, N. Sano, T. Enomoto *et al.*, 2011 Global analysis of core histones reveals nucleosomal surfaces required for chromosome bi-orientation. EMBO J. 30: 3353–3367.

Kupiec, M., 2014 Biology of telomeres: lessons from budding yeast. FEMS Microbiol. Rev. 38: 144–171.

Kurat, C. F., J. Recht, E. Radovani, T. Durbic, B. Andrews *et al.*, 2014 Regulation of histone gene transcription in yeast. Cell. Mol. Life Sci. 71: 599–613.

Li, M., and Y. Fang, 2015 Histone variants: the artists of eukaryotic chromatin. Sci. China Life Sci. 58: 232–239.

Liang, D., S. L. Burkhart, R. K. Singh, M. H. Kabbaj, and A. Gunjan, 2012 Histone dosage regulates DNA damage sensitivity in a checkpoint-independent manner by the homologous recombination pathway. Nucleic Acids Res. 40: 9604–9620.

Lomonte, P., K. F. Sullivan, and R. D. Everett, 2001 Degradation of nucleosome-associated centromeric histone H3-like protein CENP-A induced by herpes simplex virus type 1 protein ICP0. J. Biol. Chem. 276: 5829–5835.

Longtine, M. S., A. McKenzie, III, D. J. Demarini, N. G. Shah, A. Wach *et al.*, 1998 Additional modules for versatile and economical PCR-based gene deletion and modification in *Saccharomyces cerevisiae*. Yeast 14: 953–961.

Luger, K., A. W. Mader, R. K. Richmond, D. F. Sargent, and T. J. Richmond, 1997 Crystal structure of the nucleosome core particle at 2.8 A resolution. Nature 389: 251–260.

Minshull, J., A. Straight, A. Rudner, A. Dernburg, A. Belmont *et al.*, 1996 Protein phosphatase 2A regulates MPF activity and sister chromatid cohesion in budding yeast. Curr. Biol. 6: 1609–1620.

Moreno-Moreno, O., M. Torras-Llort, and F. Azorin, 2006 Proteolysis restricts localization of CID, the centromere-specific histone H3 variant of *Drosophila*, to centromeres. Nucleic Acids Res. 34: 6247–6255.

Moreno-Moreno, O., S. Medina-Giró, M. Torras-Llort, and F. Azorín, 2011 The F box protein partner of paired regulates stability of *Drosophila* centromeric histone H3, CenH3^{CID}. Curr. Biol. 21: 1488–1493.

Ng, T. M., W. G. Waples, B. D. Lavoie, and S. Biggins, 2009 Pericentromeric sister chromatid cohesion promotes kinetochore biorientation. Mol. Biol. Cell 20: 3818–3827.

Ng, T. M., T. L. Lenstra, N. Duggan, S. Jiang, S. Ceto *et al.*, 2013 Kinetochore function and chromosome segregation rely on critical residues in histones H3 and H4 in budding yeast. Genetics 195: 795–807.

Nguyen, H. T., W. Wharton, II, J. A. Harper, J. R. Dornhoffer, and A. A. Duina, 2013 A nucleosomal region important for ensuring proper interactions between the transcription elongation factor Spt16 and transcribed genes in *Saccharomyces cerevisiae*. G3 (Bethesda) 3: 929–940.

Ohkuni, K., R. Abdulle, and K. Kitagawa, 2014 Degradation of centromeric histone H3 variant Cse4 requires the Fpr3 peptidyl-prolyl c*is-trans* isomerase. Genetics 196: 1041–1045.

Ohkuni, K., Y. Takahashi, A. Fulp, J. Lawrimore, W. C. Au *et al.*, 2016 SUMO-Targeted Ubiquitin Ligase (STUbL) Slx5 regulates proteolysis of centromeric histone H3 variant Cse4 and prevents its mislocalization to euchromatin. Mol. Biol. Cell 27: 1500–1510.

Palmer, D. K., K. O'Day, M. H. Wener, B. S. Andrews, and R. L. Margolis, 1987 A 17-kD centromere protein (CENP-A) copurifies with nucleosome core particles and with histones. J. Cell Biol. 104: 805–815.

Rando, O. J., and F. Winston, 2012 Chromatin and transcription in yeast. Genetics 190: 351–387.

Ranjitkar, P., M. O. Press, X. Yi, R. Baker, M. J. MacCoss *et al.*, 2010 An E3 ubiquitin ligase prevents ectopic localization of the centromeric histone H3 variant via the centromere targeting domain. Mol. Cell 40: 455–464.

Rose, M. D., F. Winston, and P. Heiter, 1990 *Methods in Yeast Genetics*. Cold Spring Harbor Laboratory Press, Cold Spring Harbor, NY.

Sekulic, N., E. A. Bassett, D. J. Rogers, and B. E. Black, 2010 The structure of (CENP-A-H4)2 reveals physical features that mark centromeres. Nature 467: 347–351.

Sharp, J. A., A. A. Franco, M. A. Osley, and P. D. Kaufman, 2002 Chromatin assembly factor I and Hir proteins contribute to building functional kinetochores in *S. cerevisiae*. Genes Dev. 16: 85–100.

Sherman, F., G. Fink, and C. Lawrence, 1974 *Methods in Yeast Genetics*. Cold Spring Harbor Laboratory Press, Cold Spring Harbor, NY.

Singh, R. K., M.-H. M. Kabbaj, J. Paik, and A. Gunjan, 2009 Histone levels are regulated by phosphorylation and ubiquitylation-dependent proteolysis. Nat. Cell Biol. 11: 925–933.

Smith, M. M., P. Yang, M. S. Santisteban, P. W. Boone, A. T. Goldstein *et al.*, 1996 A novel histone H4 mutant defective in nuclear division and mitotic chromosome transmission. Mol. Cell. Biol. 16: 1017–1026.

Stoler, S., K. C. Keith, K. E. Curnick, and M. Fitzgerald-Hayes, 1995 A mutation in *CSE4*, an essential gene encoding a novel chromatin-associated protein in yeast, causes chromosome nondisjunction and cell cycle arrest at mitosis. Genes Dev. 9: 573–586.

Straight, A. F., A. S. Belmont, C. C. Robinett, and A. W. Murray, 1996 GFP tagging of budding yeast chromosomes reveals that protein-protein interactions can mediate sister chromatid cohesion. Curr. Biol. 6: 1599–1608.

Tachiwana, H., W. Kagawa, T. Shiga, A. Osakabe, Y. Miya *et al.*, 2011 Crystal structure of the human centromeric nucleosome containing CENP-A. Nature 476: 232–235.

Tomonaga, T., K. Matsushita, S. Yamaguchi, T. Oohashi, H. Shimada *et al.*, 2003 Overexpression and mistargeting of centromere protein-A in human primary colorectal cancer. Cancer Res. 63: 3511–3516.

Van Hooser, A. A., I. I. Ouspenski, H. C. Gregson, D. A. Starr, T. J. Yen *et al.*, 2001 Specification of kinetochore-forming chromatin by the histone H3 variant CENP-A. J. Cell Sci. 114: 3529–3542.

Venkatesh, S., and J. L. Workman, 2015 Histone exchange, chromatin structure and the regulation of transcription. Nat. Rev. Mol. Cell Biol. 16: 178–189.

Verdaasdonk, J. S., and K. Bloom, 2011 Centromeres: unique chromatin structures that drive chromosome segregation. Nature Publishing Group 12: 320–332.

White, C. L., R. K. Suto, and K. Luger, 2001 Structure of the yeast nucleosome core particle reveals fundamental changes in internucleosome interactions. EMBO J. 20: 5207–5218.

Communicating editor: J. Surtees

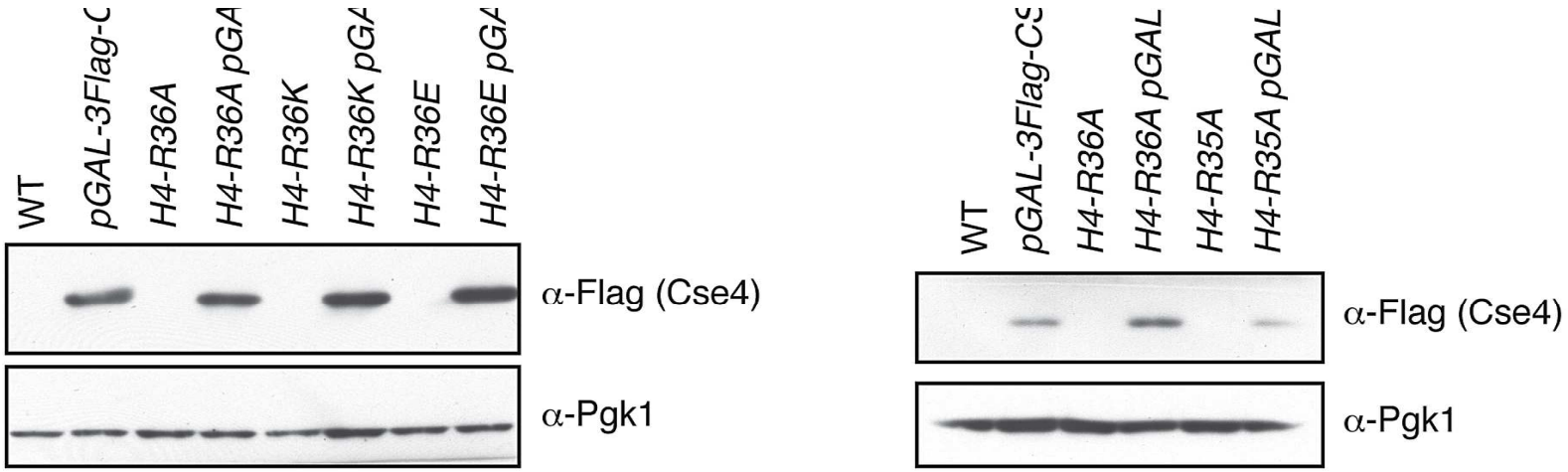

C

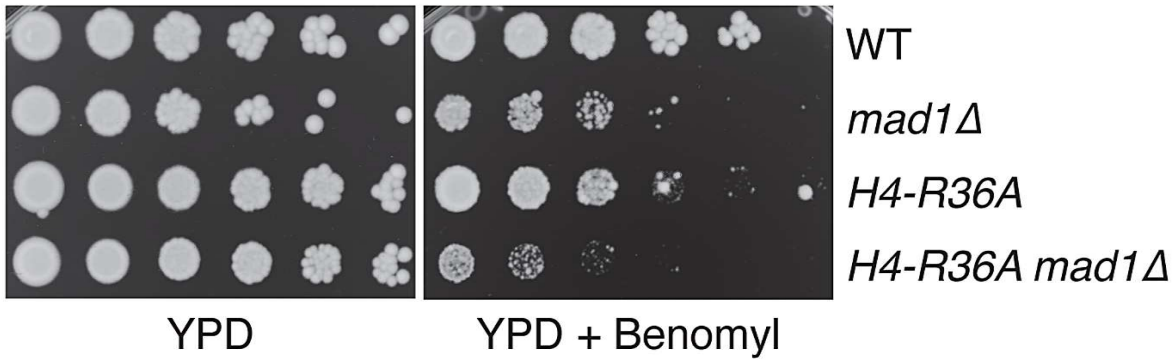

Figure S1

(A) Immunoblots of overexpressed 3Flag-Cse4 in the following strains (WT (SBY13389), *pGAL-3Flag-CSE4* (SBY13390), *H4-R36A* (SBY13391), *H4-R36A pGAL-3Flag-CSE4* (SBY13392), *H4-R36K* (SBY13393), *H4-R36K pGAL-3Flag-CSE4* (SBY13394), *H4-R36E* (SBY13395), *H4-R36E pGAL-3Flag-CSE4* (SBY13396)), corresponding to the serial dilution assay in Figure 1A. Pgk1 serves as a loading control. (B) Immunoblots of overexpressed 3Flag-Cse4 in the following strains (WT (SBY9401),

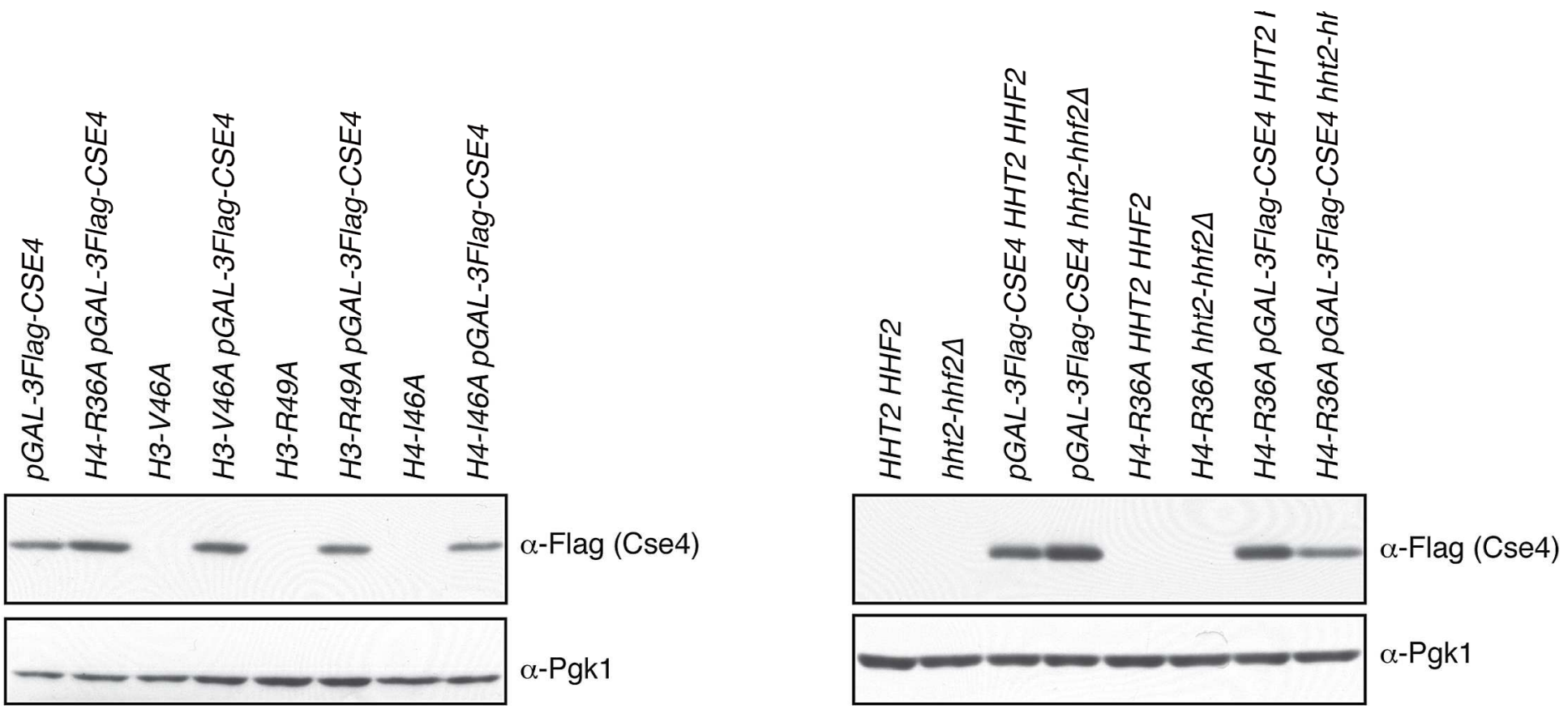

Figure S2

(A) Immunoblots of overexpressed 3Flag-Cse4 in the following strains (*pGAL-3Flag-CSE4* (SBY10025), *H4-R36A pGAL-3Flag-CSE4* (SBY9397), *H3-V46A* (SBY10392), *H3-V46A pGAL-3Flag-CSE4* (SBY10511), *H3-R49A* (SBY10393), *H3-R49A pGAL-3Flag-CSE4* (SBY10512), *H4-I46A* (SBY10394), *H4-I46A pGAL-3Flag-CSE4* (SBY10513)), corresponding to the serial dilution assay in Figure 3A. Pgk1 serves as a loading control. (B) Immunoblots of overexpressed 3Flag-Cse4 in the following strains (*HHT2-HHF2* (SBY9401), *hht2-hhf2Δ* (SBY10730), *pGAL-3Flag-CSE4 HHT2-HHF2* (SBY10025), *pGAL-3Flag-CSE4 hht2-hhf2Δ* (SBY10734), *H4-R36A HHT2-HHF2* (SBY9365), *H4-R36A hht2-hhf2Δ* (SBY10778), *H4-R36A pGAL-3Flag-CSE4 HHT2-HHF2* (SBY9397), *H4-R36A pGAL-3Flag-CSE4*

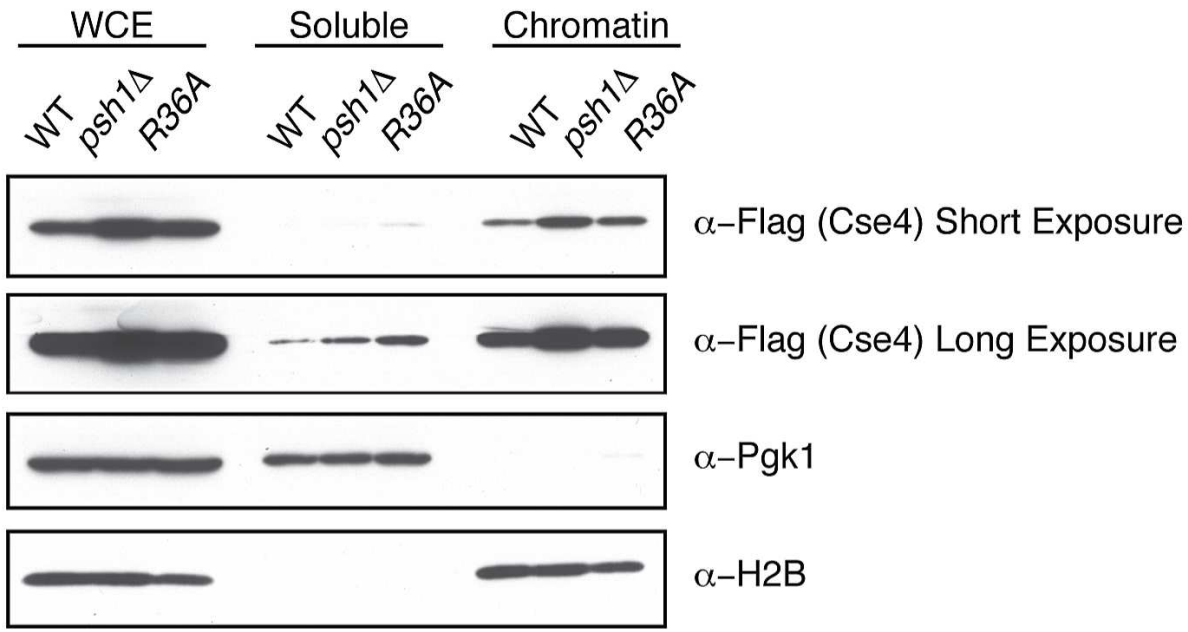

Figure S3

Chromatin fractionation from Figure 4A with a long exposure of the Flag-Cse4 blot to detect Cse4 in the soluble fraction. Whole cell extracts (WCE) from WT (SBY10025), *psh1Δ* (SBY10590), and *H4-R36A* (SBY9397) cells expressing *pGAL-3Flag-CSE4* were fractionated into soluble and chromatin fractions. 3Flag-Cse4 levels were monitored in each fraction with α-Flag antibodies. Pgk1 and H2B are markers of the soluble and chromatin fractions, respectively.

S1 Table. Plasmids used for this study.

Plasmid Number	Description	Source
pAFS52	*LacO(256), TRP1* (integrating)	(STRAIGHT *et al.* 1996)
pSB116	*pHIS3-pCUP1-GFP12-LacI12, HIS3* (integrating)	(BIGGINS *et al.* 1999)
pSB1665	*pGAL-3Flag-CSE4, URA3 (*integrating*)*	(RANJITKAR *et al.* 2010)
pSB1673	*H4 synthetic WT HYG (HHT1-HHF1* integrating*), chloramphenicol* [1]	Gift from J. Dai
pSB1729	*pGAL-3Flag-CSE4*, *LEU2* (integrating)	(HILDEBRAND AND BIGGINS 2016)
pSB1730	*2 micron, LEU2, pGAL-3Flag-CSE4*	This study
pSB1749	*H4-R36A (HHT1-HHF1* integrating*), HYG, chloramphenicol* [1]	Gift from J. Dai
pSB2576	H3-R49A (*HHT1-HHF1* integrating), HYG, chloramphenicol [1]	Gift from J. Dai
pSB2577	*H3-V46A (HHT1-HHF1* integrating*), HYG, chloramphenicol* [1]	Gift from J. Dai
pSB2578	*H3-R49A (HHT2-HHF2* integrating*), URA, amp* [2]	(DAI *et al.* 2008)
pSB2579	*H3-V46A (HHT2-HHF2* integrating*), URA, amp* [2]	(DAI *et al.* 2008)
pSB2580	*H4-R36K (HHT1-HHF1* integrating*), HYG, chloramphenicol* [1]	Gift from J. Dai
pSB2581	*H4-R36E (HHT1-HHF1* integrating*), HYG, chloramphenicol* [1]	Gift from J. Dai
pSB2582	*H4-R36K* (*HHT2-HHF2* integrating), URA, amp [2]	(DAI *et al.* 2008)
pSB2583	*H4-R36E (HHT2-HHF2* integrating*), URA, amp* [2]	(DAI *et al.* 2008)
pSB2584	*H4 synthetic WT (HHT2-HHF2* integrating*) URA amp* [2]	(DAI *et al.* 2008)
pSB2585	*H4-R36A (HHT2-HHF2* integrating*), URA, amp* [2]	(DAI *et al.* 2008)

pSB2586	*H4-I46A (HHT1-HHF1* integrating*), HYG, chloramphenicol* [1]	Gift from J. Dai
pSB2587	*H4-R35A (HHT1-HHF1* integrating*), HYG, chloramphenicol* [1]	Gift from J. Dai
pSB2588	*H4-I46A (HHT2-HHF2* integrating*), URA, amp* [2]	(DAI *et al.* 2008)
pSB2589	*H4-R35A (HHT2-HHF2* integrating*), URA, amp* [2]	(DAI *et al.* 2008)
pSB830	*2 micron, LEU2, pGAL-Myc-CSE4*	(COLLINS *et al.* 2004)
YEplac181	*2 micron, LEU2*	(GIETZ AND SUGINO 1988)

References

Biggins, S., F. F. Severin, N. Bhalla, I. Sassoon, A. A. Hyman *et al.*, 1999 The conserved protein kinase Ipl1 regulates microtubule binding to kinetochores in budding yeast. Genes Dev. 13**:** 532-544.

Collins, K. A., S. Furuyama and S. Biggins, 2004 Proteolysis contributes to the exclusive centromere localization of the yeast Cse4/CENP-A histone H3 variant. Curr Biol. 14**:** 1968-1972.

Dai, J., E. M. Hyland, D. S. Yuan, H. Huang, J. S. Bader *et al.*, 2008 Probing nucleosome function: a highly versatile library of synthetic histone H3 and H4 mutants. Cell. 134**:** 1066-1078.

Gietz, R. D., and A. Sugino, 1988 New yeast-*Escherichia coli* shuttle vectors constructed with *in vitro* mutagenized yeast genes lacking six-base pair restriction sites. Gene. 74**:** 527-534.

Hildebrand, E. M., and S. Biggins, 2016 Regulation of budding yeast CENP-A levels prevents misincorporation at promoter nucleosomes and transcriptional defects. PLoS Genet. 12**:** e1005930.

Ranjitkar, P., M. O. Press, X. Yi, R. Baker, M. J. MacCoss *et al.*, 2010 An E3 ubiquitin ligase prevents ectopic localization of the centromeric histone H3 variant via the centromere targeting domain. Molecular Cell. 40**:** 455-464.

Straight, A. F., A. S. Belmont, C. C. Robinett and A. W. Murray, 1996 GFP tagging of budding yeast chromosomes reveals that protein-protein interactions can mediate sister chromatid cohesion. Curr. Biol. 6**:** 1599-1608.

---

[1] From Histone Mutant Library version 3.0 (HMLv3.0). Kind gift from Junbiao Dai, Tsinghua University

[2] From Histone Mutant Library version 2.1 (HMLv2.1). Dai, J., E. M. Hyland, D. S. Yuan, H. Huang, J. S. Bader *et al.*, 2008 Probing nucleosome function: a highly versatile library of synthetic histone H3 and H4 mutants. Cell. 134**:** 1066-1078.

S2 Table. Yeast Strains used in this study.

All strains are isogenic with W303

Strain	Genotype	Integrated and [replicating] plasmids
SBY3	*MATa ura3-1 leu2,3-112 his3-11 trp1-1 ade2-1 can1-100 bar1-1 rad5-535*	
SBY3256	*MATa ura3-1 leu2,3-112 his3-11 trp1-1 ade2-1 can1-100 bar1-1 rad5-535 mad1::HIS3*	
SBY9365	*MATα ura3-1 leu2,3-112 his3-11 trp1-1 ade2-1 can1-100 bar1-1 rad5-535 hht1-hhf1::HHT1-synthetic-hhf1-R36A:HYG hht2-hhf2::HHT2-synthetic-hhf2-R36A:URA3*	pSB1749, pSB2585
SBY9397	*MATα ura3-1::pGAL-3Flag-CSE4:URA3 leu2,3-112 his3-11 trp1-1 ade2-1 can1-100 bar1-1 rad5-535 hht1-hhf1::HHT1-synthetic-hhf1-R36A:HYG hht2-hhf2::HHT2-synthetic-hhf2-R36A:URA3*	pSB1665, pSB1749, pSB2585
SBY9401	*MATa ura3-1 leu2,3-112 his3-11 trp1-1 ade2-1 can1-100 bar1-1 rad5-535 hht1-hhf1::HHT1-synthetic-HHF1-synthetic:HYG hht2-hhf2::HHT2-synthetic-HHF2-synthetic:URA3*	pSB1673, pSB2584
SBY9566	*MAT**α** ura3-1::pGAL-3Flag-CSE4:URA3 leu2,3-112 his3-11::pCUP1-GFP12-LacI12:HIS3 trp1-1::LacO(256 repeats):TRP1 ade2-1 can1-100 bar1-1 hht1-hhf1::HHT1-synthetic-hhf1-R36A:HYG hht2-hhf2::HHT2-synthetic-hhf2-R36A:URA3 mad1::HIS3*	pSB1665, pAFS52, pSB116, pSB1749, pSB2585
SBY9979	*MATa ura3-1 leu2,3-112 his3-11 trp1-1 ade2-1 can1-100 bar1-1 rad5-535 hht1-hhf1::HHT1-synthetic-hhf1-R36A:HYG hht2-hhf2::HHT2-synthetic-hhf2-R36A:URA3*	pSB1749, pSB2585
SBY10025	*MAT**α** ura3-1::pGAL-3Flag-CSE4:URA3 leu2,3-112 his3-11 trp1-1 ade2-1 can1-100 bar1-1 rad5-535 hht1-hhf1::HHT1-synthetic-*	pSB1665 pSB1673,

	HHF1-synthetic:HYG hht2-hhf2::HHT2-synthetic-HHF2-synthetic:URA3	pSB2584
SBY10391	*MAT**α** ura3-1::pGAL-3Flag-CSE4:URA3 leu2,3-112 his3-11::pCUP1-GFP12-LacI12:HIS3 trp1-1::LacO(256 repeats):TRP1 ade2-1 can1-100 bar1-1 hht1-hhf1::HHT1-synthetic-hhf1-R36A:HYG hht2-hhf2::HHT2-synthetic-hhf2-R36A:URA3 mad1::HIS3*	pSB1665, pAFS52, pSB116, pSB1749, pSB2585
SBY10392	*MAT**α** ura3-1 leu2,3-112 his3-11 trp1-1 ade2-1 can1-100 bar1-1 rad5-535 hht1-hhf1::hht1-V46A-HHF1-synthetic:HYG hht2-hhf2::hht2-V46A-HHF2-synthetic:URA3*	pSB2577, pSB2579
SBY10393	*MAT**α** ura3-1 leu2,3-112 his3-11 trp1-1 ade2-1 can1-100 bar1-1 rad5-535 hht1-hhf1::hht1-R49A-HHF1-synthetic:HYG hht2-hhf2::hht2-R49A-HHF2-synthetic:URA3*	pSB2576, pSB2578
SBY10394	*MAT**α** ura3-1 leu2,3-112 his3-11 trp1-1 ade2-1 can1-100 bar1-1 rad5-535 hht1-hhf1::HHT1-synthetic-hhf1-I46A:HYG hht2-hhf2::HHT2-synthetic-hhf2-I46A:URA*	pSB2586, pSB2588
SBY10450	*MAT**α** ura3-1::pGAL-3Flag-CSE4:URA3 leu2,3-112 his3-11 trp1-1 ade2-1 can1-100 bar1-1 rad5-535 hht1-hhf1::HHT1-synthetic-HHF1-synthetic:HYG hht2-hhf2::HHT2-synthetic-HHF2-synthetic:URA3 DSN1-3HA:HIS3 MTW1-13Myc:KanMX*	pSB1665, pSB1673, pSB2584
SBY10453	*MAT**α** ura3-1::pGAL-3Flag-CSE4:URA3 leu2,3-112 his3-11 trp1-1 ade2-1 can1-100 bar1-1 rad5-535 hht1-hhf1::HHT1-synthetic-hhf1-R36A:HYG hht2-hhf2::HHT2-synthetic-hhf2-R36A:UR3A DSN1-3HA:HIS3 MTW1-13Myc:KanMX*	pSB1665, pSB1749, pSB2585
SBY10494	*MAT**α** ura3-1::pGAL-3Flag-CSE4:URA3 leu2,3-112 his3-11::pCUP1-GFP12-LacI12:HIS3 trp1-1::LacO(256 repeats):TRP1 ade2-1 can1-100 bar1-1 hht1-hhf1::HHT1-synthetic-HHF1-synthetic:HYG hht2-hhf2::HHT2-synthetic-HHF2-synthetic:URA3*	pSB1665, pAFS52, pSB116, pSB1673,

	mad1::HIS3	pSB2584
SBY10510	*MAT**α** ura3-1 leu2,3-112 his3-11 trp1-1 ade2-1 can1-100 bar1-1 -535 hht1-hhf1::HHT1**-**synthetic-hhf1-R35A:HYG hht2-hhf2::HHT2**-**synthetic-hhf2-R35A:URA3*	pSB2587, pSB2589
SBY10511	*MAT**α** ura3-1::pGAL-3Flag-CSE4:URA3 leu2,3-112 his3-11 trp1-1 ade2-1 can1-100 bar1-1-535 hht1-hhf1::hht1-V46A-HHF1-synthetic:HYG hht2-hhf2::hht2-V46A-HHF2-synthetic:URA3*	pSB1665, pSB2577, pSB2579
SBY10512	*MAT**α** ura3-1::pGAL-3Flag-CSE4:URA3 leu2,3-112 his3-11 trp1-1 ade2-1 can1-100 bar1-1 rad5-535 hht1-hhf1::hht1-R49A-HHF1-synthetic:HYG hht2-hhf2::hht2-R49A-HHF2-synthetic:URA3*	pSB1665, pSB2576, pSB2578
SBY10513	*MAT**α** ura3-1::pGAL-3Flag-CSE4:URA3 leu2,3-112 his3-11 trp1-1 ade2-1 can1-100 bar1-1 rad5-535 hht1-hhf1::HHT1-synthetic-hhf1-I46A:HYG hht2-hhf2::HHT2-synthetic-hhf2-I46A:URA3*	pSB1665, pSB2586, pSB2588
SBY10590	*MAT**α** ura3-1::pGAL-3Flag-CSE4:URA3 leu2,3-112 his3-11 trp1-1 ade2-1 can1-100 bar1-1 rad5-535 hht1-hhf1::HHT1-synthetic-HHF1-synthetic:HYG hht2-hhf2::HHT2-synthetic-HHF2-synthetic:URA3 psh1::KanMX*	pSB1665, pSB1673, pSB2584
SBY10730	*MAT**α** ura3-1 leu2,3-112 his3-11 trp1-1 ade2-1 can1-100 bar1-1 rad5-535 hht1-hhf1::HHT1**-**synthetic-HHF1**-**synthetic:HYG hht2-hhf2::NAT*	pSB1673
SBY10734	*MAT**α** ura3-1::pGAL-3Flag-CSE4:URA3 leu2,3-112 his3-11 trp1-1 ade2-1 can1-100 bar1-1 rad5-535 hht1-hhf1::HHT1-synthetic-HHF1-synthetic:HYG hht2-hhf2::NAT*	pSB1665, pSB1673
SBY10778	*MAT**α** ura3-1 leu2,3-112 his3-11 trp1-1 ade2-1 can1-100 bar1-1 rad5-535 hht1-hhf1::HHT1-synthetic-hhf1-R36A:HYG hht2-hhf2::NAT*	pSB1749
SBY10782	*MAT**α** ura3-1::pGAL-3Flag-CSE4:URA3 leu2,3-112 his3-11 trp1-1 ade2-1 can1-100 bar1-1 rad5-535 hht1-hhf1::HHT1-synthetic-*	pSB1665, pSB1749

	hhf1-R36A:HYG hht2-hhf2::NAT	
SBY11189	*MATa ura3-1 leu2,3-112::pGAL-3Flag-CSE4:LEU2 his3-11 trp1-1 ade2-1 can1-100 bar1-1 rad5-535 psh1::KanMX*	pSB1729
SBY13213	*MAT**α** ura3-1::pGAL-3Flag-CSE4:URA3 leu2,3-112 his3-11 trp1-1 ade2-1 can1-100 bar1-1 rad5-535 hht1-hhf1::HHT1-synthetic-HHF1-synthetic:HYG hht2-hhf2::HHT2-synthetic-HHF2-synthetic:URA3 Psh1-13Myc::HIS3*	pSB1665, pSB1673, pSB2584
SBY13215	*MAT**α** ura3-1::pGAL-3Flag-CSE4:URA3 leu2,3-112 his3-11 trp1-1 ade2-1 can1-100 bar1-1 rad5-535 hht1-hhf1::HHT1-synthetic-hhf1-R36A:HYG hht2-hhf2::HHT2-synthetic-hhf2-R36A:URA3 Psh1-13Myc::HIS3*	pSB1665, pSB1749, pSB2585
SBY13389	*MATa ura3-1 leu2,3-112 his3-11 trp1-1 ade2-1 can1-100 bar1-1 rad5-535 hht1-hhf1::HHT1-synthetic-HHF1 synthetic:HYG hht2-hhf2::HHT2-synthetic-HHF2 synthetic:URA3 [2 micron, LEU2]*	[pSB291], pSB1673, pSB2584
SBY13390	*MATa ura3-1 leu2,3-112 his3-11 trp1-1 ade2-1 can1-100 bar1-1 rad5-535 hht1-hhf1::HHT1-synthetic-HHF1 synthetic:HYG hht2-hhf2::HHT2-synthetic-HHF2 synthetic:URA3 [2 micron, LEU2, pGAL-3Flag-CSE4]*	[pSB1730], pSB1673, pSB2584
SBY13391	*MAT**α** ura3-1 leu2,3-112 his3-11 trp1-1 ade2-1 can1-100 bar1-1 rad5-535 hht1-hhf1::HHT1-synthetic-hhf1-R36A:HYG hht2-hhf2::HHT2-synthetic-hhf2-R36A:URA3 [2 micron, LEU2]*	[pSB291], pSB1749, pSB2585
SBY13392	*MAT**α** ura3-1 leu2,3-112 his3-11 trp1-1 ade2-1 can1-100 bar1-1 rad5-535 hht1-hhf1::HHT1-synthetic-hhf1-R36A:HYG hht2-hhf2::HHT2-synthetic-hhf2-R36A:URA3 [2 micron, LEU2, pGAL-3Flag-CSE4]*	[pSB1730], pSB1749, pSB2585
SBY13393	*MATa ura3-1 leu2,3-112 his3-11 trp1-1 ade2-1 can1-100 bar1-1 rad5-535 hht1-hhf1::HHT1-synthetic-hhf1-R36K:HYG hht2-hhf2::HHT2-synthetic-hhf2-R36K:URA3 [2 micron, LEU2]*	[pSB291], pSB2580, pSB2582

SBY13394	*MATa ura3-1 leu2,3-112 his3-11 trp1-1 ade2-1 can1-100 bar1-1 rad5-535 hht1-hhf1::HHT1-synthetic-hhf1-R36K:HYG hht2-hhf2::HHT2-synthetic-hhf2-R36K:URA3 [2 micron, LEU2, pGAL-3Flag-CSE4]*	[pSB1730], pSB2580, pSB2582
SBY13395	*MAT**α** ura3-1 leu2,3-112 his3-11 trp1-1 ade2-1 can1-100 bar1-1 rad5-535 hht1-hhf1::HHT1-synthetic-hhf1-R36E:HYG hht2-hhf2::HHT2-synthetic-hhf2-R36E:URA3 [2 micron, LEU2]*	[pSB291], pSB2581, pSB2583
SBY13396	*MAT**α** ura3-1 leu2,3-112 his3-11 trp1-1 ade2-1 can1-100 bar1-1 rad5-535 hht1-hhf1::HHT1-synthetic-hhf1-R36E:HYG hht2-hhf2::HHT2-synthetic-hhf2-R36E:URA3 [2 micron, LEU2, pGAL-3Flag-CSE4]*	[pSB1730], pSB2581, pSB2583
SBY13407	*MAT**α** ura3-1::pGAL-3Flag-CSE4:URA3 leu2,3-112 his3-11 trp1-1 ade2-1 can1-100 bar1-1 rad5-535 hht1-hhf1::HHT1-synthetic-hhf1-R36K:HYG hht2-hhf2::HHT2-synthetic-hhf2-R36K:URA3*	pSB1665, pSB2580, pSB2582
SBY13723	*MATa ura3-1 leu2,3-112 his3-11 trp1-1 ade2-1 can1-100 bar1-1 rad5-535 hht1-hhf1::HHT1-synthetic-HHF1-synthetic:HYG hht2-hhf2::HHT2-synthetic-HHF2-synthetic:URA3 PSH1-3Flag:TRP1*	pSB1673, pSB2584
SBY13725	*MATa ura3-1 leu2,3-112 his3-11 trp1-1 ade2-1 can1-100 bar1-1 rad5-535 hht1-hhf1::HHT1-synthetic-hhf1-R36A:HYG hht2-hhf2::HHT2-synthetic-hhf2-R36A:URA3 PSH1-3Flag:TRP1*	pSB1749, pSB2585
SBY13729	*MAT**α** ura3-1::pGAL-3Flag-CSE4:URA3 leu2,3-112 his3-11::pCUP1-GFP12-LacI12:HIS3 trp1-1::LacO(256 repeats):TRP1 ade2-1 can1-100 bar1-1 hht1-hhf1::HHT1-synthetic-HHF1-synthetic:HYG hht2-hhf2::HHT2-synthetic-HHF2-synthetic:URA3*	pSB1665, pAFS52, pSB116, pSB1673, pSB2584
SBY13812	*MATa ura3-1 leu2,3-112::pGAL-3Flag-CSE4:LEU2 his3-11 trp1-1 ade2-1 can1-100 bar1-1 rad5-535 hht1-hhf1::HHT1-synthetic-hhf1-R36A:HYG hht2-hhf2::HHT2-synthetic-hhf2-R36A:URA3*	pSB1729, pSB1749, pSB2585

SBY15335	*MATa ura3-1 leu2,3-112 his3-11 trp1-1 ade2-1 can1-100 bar1-1 rad5-535 hht1-hhf1::HHT1-synthetic-HHF1-synthetic:HYG hht2-hhf2::HHT2-synthetic-HHF2-synthetic:URA3 PSH1-13Myc:HIS3 SPT16-3Flag:KanMX*	pSB1673, pSB2584
SBY15624	*MATa ura3-1 leu2,3-112 his3-11 trp1-1 ade2-1 can1-100 bar1-1 rad5-535 hht1-hhf1::HHT1-synthetic-hhf1-R36A:HYG hht2-hhf2::HHT2-synthetic-hhf2-R36A:URA3 PSH1-13Myc:HIS3 SPT16-3Flag:KanMX*	pSB1749, pSB2585
SBY16468	*MATa ura3-1 leu2,3-112 his3-11 trp1-1 ade2-1 can1-100 bar1-1 rad5-535 hht1-hhf1::HHT1-synthetic-hhf1-R36K:HYG hht2-hhf2::HHT2-synthetic-hhf2-R36K:URA3 PSH1-13Myc:HIS3 SPT16-3Flag:KanMX*	pSB2580, pSB2582
SBY16469	*MAT**α** ura3-1 leu2,3-112::pGAL-3Flag-CSE4:LEU2 his3-11 trp1-1 ade2-1 can1-100 bar1-1 rad5-535 hht1-hhf1::HHT1-synthetic-HHF1-synthetic:HYG hht2-hhf2::HHT2-synthetic-HHF2-synthetic:URA3*	pSB1729, pSB1673, pSB2584
SBY16594	*MATa ura3-1 leu2,3-112 his3-11 trp1-1 ade2-1 can1-100 bar1-1 rad5-535 hht1-hhf1::HHT1-synthetic-hhf1-R36K:HYG hht2-hhf2::HHT2-synthetic-hhf2-R36K:URA3 PSH1-3Flag:TRP1*	pSB2580, pSB2582

S3 Table. Oligonucleotides used for this study.

Oligo Number	Purpose	Sequence (5' to 3')	Source
FO1798 (SB4470)	*ADH1* gene Forward	ACGCTTGGCACGGTGACTG	(DUINA *et al.* 2007)
FO1800 (SB4471)	*ADH1* gene Reverse	ACCGTCGTGGGTGTAACCAGA	(DUINA *et al.* 2007)
FO1803 (SB4472)	*ADH1* 3' Forward	CCCAACTGAAGGCTAGGCTGTGG	(DUINA *et al.* 2007)
FO1804 (SB4473)	*ADH1* 3' Reverse	ACCGGCATGCCGAGCAAATGCCTG	(DUINA *et al.* 2007)
FO1814 (SB4076)	*PMA1* gene Forward	CTATTATTGATGCTTTGAAGACCTCCAG	(DUINA *et al.* 2007)
FO1815 (SB4077)	*PMA1* gene Reverse	TGCCCAAAATAATAGACATACCCCATAA	(DUINA *et al.* 2007)
OAD383 (SB5027)	*PMA1* 3' Forward	CGTAAGCGAGACTTCCAAATGG	(MYERS *et al.* 2011)
OAD384 (SB5028)	*PMA1* 3' Reverse	TCCTGCCCAGCTCTTCTATAATACTT	(MYERS *et al.* 2011)
OAD394 (SB5029)	*PMA1* 5' Forward	AGTTGCCGCCGGTGAA	(MYERS *et al.* 2011)
OAD395 (SB5030)	*PMA1* 5' Reverse	CCGTAAGATGGGTCAGTTTGTAAAT	(MYERS *et al.* 2011)
SB773	*CEN3* Forward	ATCAGCGCCAAACAATATGGAAAA	(COLLINS *et al.* 2005)
SB774	*CEN3* Reverse	GAGCAAAACTTCCACCAGTAAACG	(COLLINS *et al.* 2005)
SB5059	*ADH1* 5' Forward	CGACAAAGACAGCACCAACA	This study
SB5060	*ADH1* 5' Reverse	TGTGCGTGAATGAAGGAAGG	This study

References

Collins, K. A., A. R. Castillo, S. Y. Tatsutani and S. Biggins, 2005 *De novo* kinetochore assembly requires the centromeric histone H3 variant. Mol Biol Cell. 16**:** 5649-5660.

Duina, A. A., A. Rufiange, J. Bracey, J. Hall, A. Nourani *et al.*, 2007 Evidence that the localization of the elongation factor Spt16 across transcribed genes is dependent upon histone H3 integrity in *Saccharomyces cerevisiae*. Genetics. 177**:** 101-112.

Myers, C. N., G. B. Berner, J. H. Holthoff, K. Martinez-Fonts, J. A. Harper *et al.*, 2011 Mutant versions of the *S. cerevisiae* transcription elongation factor Spt16 define regions of Spt16 that functionally interact with histone H3. PLoS One. 6**:** e20847.